THE JOURNAL OF BIOLOGICAL CHEMISTRY VOL. 284, NO. 12, pp. 7940–7950, March 20, 2009

Conversion of Wild-type α-Synuclein into Mutant-type Fibrils and Its Propagation in the Presence of A30P Mutant*[S]

Received for publication, September 26, 2008, and in revised form, January 21, 2009 Published, JBC Papers in Press, January 21, 2009, DOI 10.1074/jbc.M807482200

Motokuni Yonetani[‡§], Takashi Nonaka[‡], Masami Masuda[‡§], Yuki Inukai[‡§], Takayuki Oikawa[‡§], Shin-ichi Hisanaga[§], and Masato Hasegawa[‡1]

From the [‡]Department of Molecular Neurobiology, Tokyo Institute of Psychiatry, 2-1-8 Kamikitazawa, Setagaya-ku, 156-8585 Tokyo, Japan and the [§]Molecular Neuroscience Laboratory, Graduate School of Science and Engineering, Tokyo Metropolitan University, 1-1 Minami-Osawa, Hachioji-shi, 192-0397 Tokyo, Japan

Fibrillization or conformational change of α-synuclein is central in the pathogenesis of α-synucleinopathies, such as Parkinson disease. We found that the A30P mutant accelerates nucleation-dependent fibrillization of wild type (WT) α-synuclein. Electron microscopy observation and ultracentrifugation experiments revealed that shedding of fragments occurs from A30P fibrils and that these fragments accelerate fibrillization by serving as seeds. Immunochemical analysis using epitope-specific antibodies and biochemical analyses of protease-resistant cores demonstrated that A30P fibrils have a distinct conformation. Interestingly, WT fibrils formed with A30P seeds exhibited the same character as A30P fibrils, as did A30P fibrils formed with WT seeds, indicating that the A30P mutation affects the conformation and fibrillization of both WT and A30P. These effects of A30P mutation may explain the apparent conflict between the association of A30P with Parkinson disease and the slow fibrillization of A30P itself and therefore provide new insight into the molecular mechanisms of α-synucleinopathies.

Parkinson disease (PD)[2] is the second most common neurodegenerative disorder, after Alzheimer disease. Neuropathological features of PD are selective loss of dopaminergic neurons in the substantia nigra and appearance of intracellular inclusion bodies, referred to as Lewy bodies (LBs) and Lewy neurites. Ultrastructurally, LBs are composed of a dense core of filamentous and granular material that is surrounded by radially oriented fibrils (1, 2). Biochemical and immunochemical analyses showed that hyperphosphorylated α-synuclein is the major component of the fibrous structures of LBs and Lewy neurites (3).

Genetic analyses of α-synuclein gene of familial cases of PD and dementia with LBs have demonstrated that expression of abnormal α-synuclein or overexpression of normal α-synuclein is associated with these diseases; namely, three missense mutations (A53T (4), A30P (5), and E46K (6)) and multiplication (7–12) of the α-synuclein gene have been found to cosegregate with the onset of PD in kindreds of autosomal dominantly inherited familial PD and dementia with LBs.

α-Synuclein is a 140-amino acid protein, harboring seven imperfect tandem repeats (KTKEGV-type) in the N-terminal half, followed by a hydrophobic central region (non-Aβ component of Alzheimer disease (NAC)) and an acidic C-terminal. The tandem repeat region has been assumed to form an amphipathic α-helix by binding to phospholipid (13). Circular dichroism and Fourier-transform IR analysis revealed that α-synuclein is a natively unfolded protein with little ordered secondary structure (14). However, recent NMR analyses have revealed three intramolecular long range interactions. These interactions are between the highly hydrophobic NAC region (residues 85–95) and the C terminus (residues 110–130), C-terminal residues 120–130 and residues 105–115, and the region around residue 120 and the N terminus around residue 20 (15).

Recombinant α-synuclein *in vitro* assembles into fibrils that closely resemble those in brains with PD and dementia with LBs upon incubation at a high concentration at 37 °C with shaking, whereas other synuclein family proteins (*i.e.* β-synuclein and γ-synuclein) neither accumulate in the brain (1, 16) nor form fibrils (17–19). During the assembly of α-synuclein fibrils, conformational change from random coil to β-sheet structure can be observed. It has been shown that the sequence of the NAC region in α-synuclein is necessary for the assembly (20).

Mostly in *in vitro* experiments, it has been shown that the A53T and E46K mutations promote fibrillization (17, 21–25), whereas the effect of A30P mutation on fibrillization is unclear. It has been reported that A30P mutation promotes oligomerization of nonfibrillar protofibrils (23, 26) and that some of the protofibrils with a circular morphology may form pores by binding to ER membrane (27). It has also been reported that A30P mutation is defective in binding to phospholipid vesicles, and the alteration of membrane interaction could contribute to early onset of PD (28, 29).

* This work was supported by a Grant-in-Aid for Scientific Research on Priority Areas, Research on Pathomechanisms of Brain Disorders (to M. H.), a Grant-in-Aid for Scientific Research (B) (to M. H.), and a Grant-in-Aid for Scientific Research (C) (to M. H.) from the Ministry of Education, Culture, Sports, Science and Technology of Japan. The costs of publication of this article were defrayed in part by the payment of page charges. This article must therefore be hereby marked "*advertisement*" in accordance with 18 U.S.C. Section 1734 solely to indicate this fact.

[S] The on-line version of this article (available at http://www.jbc.org) contains supplemental Figs. 1–3.

[1] To whom correspondence should be addressed: Dept. of Molecular Neurobiology, Tokyo Institute of Psychiatry, Tokyo Metropolitan Organization for Medical Research, 2-1-8 Kamikitazawa, Setagaya-ku, Tokyo 156-8585, Japan. Tel.: 81-3-3304-5701; Fax: 81-3-3329-8035; E-mail: masato@prit.go.jp.

[2] The abbreviations used are: PD, Parkinson disease; LB, Lewy body; WT, wild type; NAC, non-Aβ component of Alzheimer disease; Th-S, thioflavin S; MOPS, 3-(*N*-morpholino)propanesulfonic acid; CBB, Coomassie Brilliant Blue; MTT, 3-(4,5-dimethylthiazol-2-yl)-2,5-diphenyltetrazolium bromide; EM, electron microscopy.

Assembly of protein into fibrils is usually a nucleation-dependent process that consists of a lag phase (nucleation) and a growth phase (elongation). α-Synuclein fibrillization was confirmed to be a nucleation-dependent process (22). The addition of seeds to the monomer promotes fibrillization by rendering the nucleation process redundant. Not only wild type (WT) fibrils but also A53T fibrils have been reported to act as nuclei for fibrillization of WT α-synuclein (30).

In this study, we have investigated nucleation-dependent fibrillization of WT and A30P α-synuclein and the conformations of WT and A30P fibrils formed in the presence of WT and A30P seeds. We found that A30P seeds accelerated the nucleation-dependent fibrillization of WT α-synuclein more effectively than did WT seeds. Further, A30P fibrils have a distinct conformation from WT fibrils and show a higher level of fragment shedding. The WT fibrils formed in the presence of A30P seeds showed the same character as A30P fibrils, suggesting that the nucleation-dependent assembly of WT fibrils in the presence of A30P seeds results in conversion of WT conformation to that of A30P. Further, the A30P fibrils formed in the presence of WT seeds shared the properties of A30P fibrils. The *in vitro* results shown here implicate the structural and functional differences among α-synuclein amyloid fibrils, useful for understanding the pathogenesis of α-synucleinopathies.

EXPERIMENTAL PROCEDURES

Antibodies—α-Synuclein epitope-specific polyclonal antibodies syn1–10, syn75–91, and syn131–140 were raised against synthetic peptides MDVFMKGLSKC (residues 1–10 with Cys at the C terminus), CTAVAQKTVEGAGSIAAA (residues 75–91 with Cys at the N terminus), and CEGYQDYEPEA (residues 131–140 with Cys at the N terminus) of human α-synuclein, respectively. Peptides were conjugated to *m*-maleimidobenzoyl-*N*-hydrosuccinimide ester-activated keyhole limpet hemocyanin. The keyhole limpet hemocyanin-peptide complex (1 mg of each immunogen) emulsified in Freund's complete adjuvant was injected subcutaneously into a New Zealand white rabbit, followed by five weekly subcutaneous injections of 150 mg of KLH-peptide complex emulsified in Freund's incomplete adjuvant starting from 3 weeks after the first immunization. Other anti-α-synuclein antibodies, number 36 (residues 1–10) and NAC2 (residues 75–91), were kindly provided by Dr. Iwatsubo and Dr. Jäkälä, respectively.

Expression and Purification of Human WT and Mutant α-Synuclein—Human α-synuclein cDNA in bacterial expression plasmid pRK172 was provided by Dr. Goedert. A30P, E46K, and A53T mutations were induced by site-directed mutagenesis (Stratagene). WT and mutant α-synuclein were expressed in *Escherichia coli* BL21 (DE3) cells and purified as described (31). Protein concentration was determined as described (31).

Fibrillization of WT and Mutant α-Synuclein—Purified WT and mutant α-synuclein (1 mg/ml) were each incubated at 37 °C, with shaking at 200 rpm in 30 mM Tris-HCl, pH 7.5, containing 0.1% NaN_3. For quantitative assessment of fibrillization, aliquots (10 μl) of assembly mixture were removed at various time points, brought to 300 μl with 5 mM Thioflavin S (Th-S) in 20 mM MOPS, pH 6.8, and incubated for 60 min at room temperature. Fluorimetry was performed using a Hitachi F4000 fluorescence spectrophotometer (set at 440 nm excitation/521 nm emission) as described (32).

Preparation of Seeds—Purified WT and mutant α-synuclein (7 mg/ml) were each incubated for 96–120 h at 37 °C, with shaking at 200 rpm in 30 mM Tris-HCl, pH 7.5, containing 0.1% NaN_3. Assembly mixture was diluted in 5 volumes of 30 mM Tris-HCl, pH 7.5, and ultracentrifuged at 151,000 × *g* for 20 min at 25 °C. The pellets were resuspended in 5 volumes of 30 mM Tris-HCl, pH 7.5, and ultracentrifuged at 151,000 × *g* for 20 min again. The pellets were resuspended homogeneously by pipetting in 30 mM Tris-HCl, pH 7.5, containing 0.1% NaN_3 and used as seeds. Aliquots of seeds or fibrils were solubilized in 6 M guanidine hydrochloride, and the concentration of α-synuclein was determined as described (31).

Nucleation-dependent Fibrillization of α-Synuclein—Purified WT or mutant α-synuclein (1 mg/ml) in 30 mM Tris-HCl, pH 7.5, containing 0.1% NaN_3 was incubated with seeds (1% of total protein) for 0–144 h at 37 °C without shaking. Fibrillization was monitored by measuring Th-S fluorescence.

Semiquantitative Analysis of Fibril Length in Suspended Fibrils—Fibrils formed in the presence or absence of seeds (0.1 mg/ml) were observed at a magnification of ×25,000 by electron microscopy after suspension by pipetting. Fibril length was measured on the photographs, and the populations were calculated.

Characterization of Seeds by Ultracentrifugation—Seeds or fibrils formed in the presence of seeds (1.0 mg/ml) were suspended in 5 volumes of 30 mM Tris-HCl, pH 7.5, and incubated for 30 min at room temperature, followed by ultracentrifugation for 20 min at 109,000 × *g*. The pellets were resuspended in equal volumes of the supernatant with 30 mM Tris-HCl, pH 7.5. The supernatant and suspension were treated with 5× SDS sample buffer and subjected to SDS-PAGE. After staining of gels with Coomassie Brilliant Blue (CBB) and scanning, the intensities of the α-synuclein band were quantified by Scion Image (Scion Corp.). Aliquots of the supernatants were examined by electron microscopy and used for studies of nucleation-dependent fibrillization.

Electron Microscopy—Fibrils, seeds and fibrils formed in the presence of seeds were diluted in 30 mM Tris-HCl, pH 7.5. Aliquots of these dilutions and centrifugal supernatants of seeds and fibrils formed in the presence of seeds were placed on 400-mesh collodion-coated grids, negatively stained with 2% lithium phosphotungstate, and observed with a JEOL 1200EXII electron microscope.

Dot Blot Assay—α-Synuclein monomer, seeds and fibrils formed in the presence of seeds were diluted in 30 mM Tris-HCl, pH 7.5, 0.1% NaN_3 and spotted onto polyvinylidene difluoride membrane. The membrane was probed with epitope-specific α-synuclein antibodies syn1–10 (N-terminal region), syn75–91 (NAC region), and syn131–140 (C-terminal region) or stained with CBB to detect total protein. Immunoreactivity was visualized using the avidin-biotin detection system (Vector Laboratories) and quantified by scanning as described above.

Comparison of Protease-resistant Cores of α-Synuclein Fibrils—Seeds or fibrils formed in the presence of seeds (1.0 mg/ml) were sonicated and treated with 50 μg/ml trypsin or 2 μg/ml

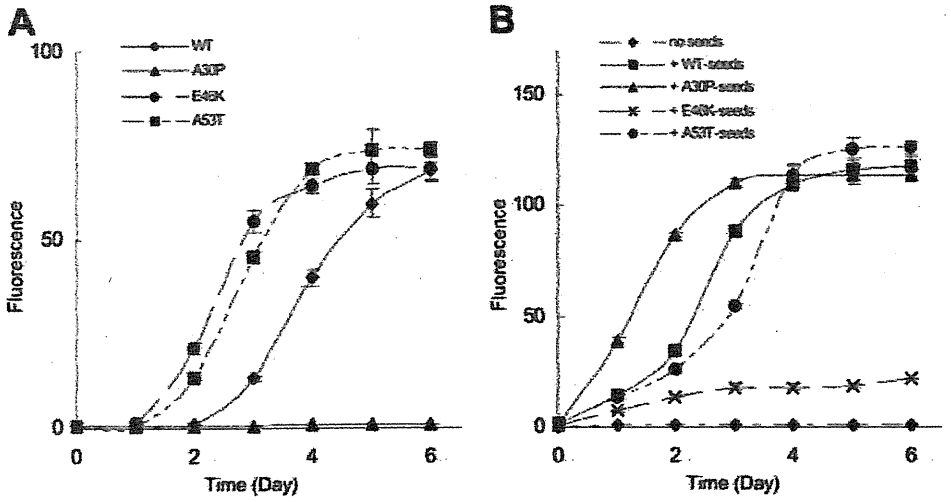

FIGURE 1. **Fibrillization of WT and mutant α-synuclein (*A*) and promotion of WT α-synuclein fibrillization by the addition of WT or mutant fibrils seeds (*B*).** *A*, WT and mutant α-synuclein (1.0 mg/ml) were incubated with shaking at 37 °C in the absence of seeds. *B*, WT α-synuclein (1.0 mg/ml) was incubated without shaking at 37 °C in the presence of WT or mutant fibril seeds (0.1% of total protein). Fibrillization was monitored by measuring the Th-S fluorescence. Results are expressed as means ± S.E. ($n = 3$).

proteinase K at 37 °C for 30 min. The reaction was stopped by boiling for 5 min. The solution was treated with sample buffer containing 2% SDS and 8 M urea and subjected to SDS-PAGE.

Cytotoxicity Assay—The cytotoxic effect of α-synuclein fibrils was assessed by measuring cellular redox activity with 3-(4,5-dimethylthiazol-2-yl)-2,5-diphenyltetrazolium bromide (MTT), as described (33). Briefly, SH-SY5Y cells cultured in a 96-well microtiter plate were treated with 500 nM α-synuclein monomer, fibrils (suspended by pipetting or sonication), or fibrils formed in the presence of seeds. Following a 6-h incubation, the cytotoxic effect was assessed by measuring cellular redox activity.

Statistical Analysis—Statistic analysis was performed using unpaired Student's *t* test. The results are expressed as means ± S.E. of three independent experiments ($n = 3$).

RESULTS

Effect of A30P Seeds on Fibrillization of α-Synuclein—First, we tested the effect of mutations on fibrillization of α-synuclein. As shown in Fig. 1*A*, both A53T and E46K mutants fibrillized faster than WT, whereas the fibrillization of A30P mutant was much slower than that of WT, confirming the previous observations. Since A53T fibrils can act as seeds for the fibrillization of WT α-synuclein (30), we next investigated whether A30P fibrils also act as seeds for WT monomer. We incubated WT α-synuclein with WT, A30P, E46K, or A53T seeds under conditions where WT α-synuclein itself does not form fibrils and analyzed fibrillization (Fig. 1*B*). Fibrillization was observed following the addition of either WT seeds or mutant seeds. Interestingly, the assembly was faster in the presence of A30P seeds than in the presence of WT or the other mutant seeds. The time required for half-maximal fibrillization was ~1.5 days with A30P seeds, which is shorter than those with the other seeds, WT (2.5 days), E46K (more than 6 days), and A53T (6 days).

In the brains of patients with the A30P mutation, both WT and A30P α-synuclein are expressed. Therefore, a mixture of WT and A30P α-synuclein was incubated with WT or A30P seeds, and the progress of fibrillization was observed in terms of Th-S fluorescence intensity. As in the case of WT α-synuclein monomer alone, A30P seeds accelerated the fibrillization process more effectively than did WT seeds (supplemental Fig. 1). Fibrillization was not observed in the absence of seeds. The time for half-maximal fibrillization was ~1.5 days with A30P seeds and 3.5 days with WT seeds.

Shedding of Fragments from A30P Fibrils—To elucidate the mechanism of the effect of A30P seeds on fibrillization, we utilized electron microscopy (Fig. 2). Many tiny or short fibrils were observed in A30P seeds, whereas relatively long fibrils were predominantly detected in WT, E46K, and A53T seeds (Fig. 2*A*, *v*, *vi*, *vii*, and *viii*). This observation was confirmed by measuring the fibril length in these seeds. Short fibrils of less than 100 nm were predominant in the A30P seeds, whereas longer fibrils were detected in the WT and A53T seeds (supplemental Fig. 3*A*). Before preparation of the seeds, WT and mutant α-synuclein fibrils were uniformly long and showed no morphological differences (Fig. 2*A*, *i*, *ii*, *iii*, and *iv*). Therefore, it appeared that A30P fibrils readily fragmented during the process of seed preparation. To test whether the small fibrils could be separated by centrifugation or not, WT and mutant α-synuclein seeds were ultracentrifuged, and the supernatants were observed by electron microscopy. Surprisingly, many tiny fibrils were observed in the supernatant of A30P seeds, whereas such tiny fibrils were hardly detected in the supernatant of WT, E46K, and A53T seeds (Fig. 2*A*, *ix*, *x*, *xi*, and *xii*), indicating that A30P fibrils have a higher propensity for shedding fragments than do WT fibrils and that the small fragments are recovered in the supernatant of ultracentrifugation.

We then attempted to quantitate the fragmented fibrils by ultracentrifugation. The centrifugal supernatant was subjected to SDS-PAGE, and the gel was stained with CBB. As expected, more α-synuclein was detected in the supernatant of A30P seeds than in those of WT, E46K, and A53T seeds (Fig. 2, *B* and *C*).

Next, we investigated whether the tiny fibrils recovered in the supernatant of ultracentrifugation can act as seeds for fibrillization of α-synuclein. WT α-synuclein was incubated with the supernatant of WT, A30P, E46K, or A53T seeds (10% of total volume), and fibrillization was monitored by a Th-S assay. In the presence of the supernatant of WT, E46K, and A53T seeds, a very slow increase of Th-S was observed, whereas fibrillization was accelerated in the presence of the supernatant of A30P seeds (Fig. 2*D*), as seen in the fibrillization in Fig. 1*B*. These results indicate that the A30P fibrils readily shed many tiny fibrils that can act as seeds for fibrillization.

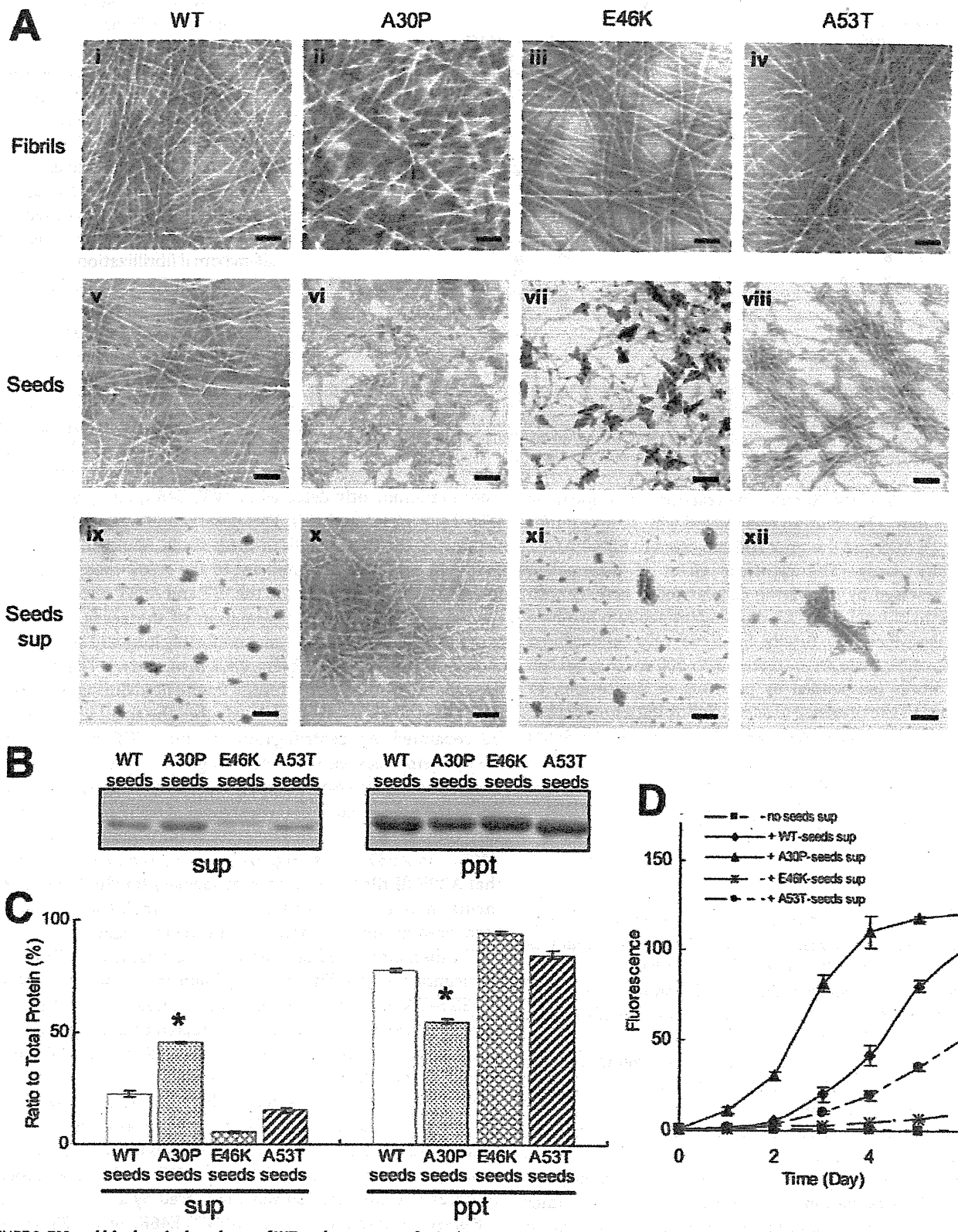

FIGURE 2. **EM and biochemical analyses of WT and mutant seeds.** *A*, electron microscopy of WT and mutant fibrils, fibril seeds, and seed supernatants (*sup*) after ultracentrifugation. Shown are fibrils (*i*, *ii*, *iii*, and *iv*), seeds (*v*, *vi*, *vii*, and *viii*), and seed supernatants (*ix*, *x*, *xi*, and *xii*) of WT (*i*, *v*, and *ix*), A30P (*ii*, *vi*, and *x*), E46K (*iii*, *vii*, and *xi*), and A53T (*iv*, *viii*, and *xii*) α-synuclein. Negatively stained fibrils, seeds, or seed supernatants were observed by electron microscopy. *Scale bar*, 200 nm. *B*, biochemical analysis of WT and mutant seeds after ultracentrifugation. Pellets and supernatants were subjected to SDS-PAGE and stained with CBB. *C*, quantification of α-synuclein recovered in the supernatants and pellets (expressed as a percentage of total α-synuclein, taken as 100%). The results are expressed as means ± S.E. ($n = 3$) (*, $p < 0.01$). *D*, WT α-synuclein monomer seeding activities of short fibrils recovered in the supernatants of ultracentrifugation. The results are expressed as means ± S.E. ($n = 3$).

Effect of A30P Mutation on Fibrillization of α-Synuclein

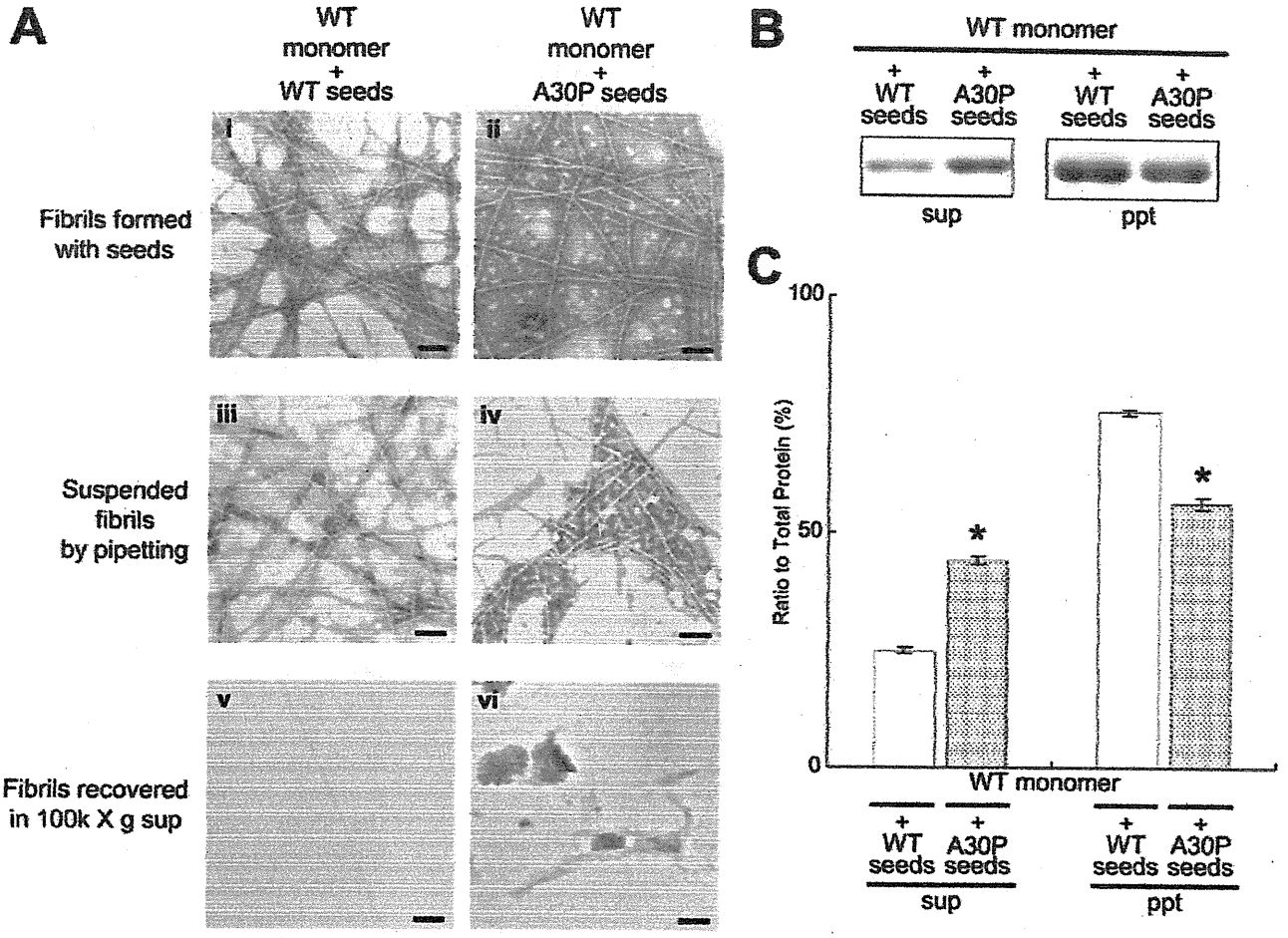

FIGURE 3. **EM and biochemical analyses of WT fibrils formed in the presence of WT or A30P seeds.** *A*, EM analysis of WT fibrils formed in the presence of WT or A30P seeds, suspended fibrils, and the supernatants after ultracentrifugation for WT fibrils formed with WT seeds (*i*, *iii*, and *v*) and WT fibrils formed with A30P seeds (*ii*, *iv*, and *vi*). Negatively stained WT fibrils formed in the presence of WT or A30P seeds (*i* and *ii*), the fibrils after suspension (*iii* and *iv*), and the fibrils in the supernatants after centrifugation (*iv* and *v*) were observed by electron microscopy. *Scale bar*, 200 nm. *B*, biochemical analysis of α-synuclein fibrils fractionated by ultracentrifugation. *C*, quantification of α-synuclein recovered in the supernatants and pellets after ultracentrifugation (expressed as a percentage of total α-synuclein, taken as 100%). The results are expressed as means ± S.E. ($n = 3$) (*, $p < 0.01$).

Shedding Property of WT Fibrils Formed in the Presence of A30P Seeds—Next, we investigated whether or not the WT fibrils formed in the presence of A30P seeds have the same properties as A30P fibrils (Fig. 3*A*). The WT fibrils formed in the presence of A30P seeds appeared to be morphologically indistinguishable from the WT fibrils formed in the presence of WT seeds before preparation of suspensions (Fig. 3*A*, *i* and *ii*). However, after suspension, many tiny fibrils were shed from WT fibrils formed in the presence of A30P seeds, whereas only a few short fibrils were shed from WT fibrils formed in the presence of WT seeds (Fig. 3*A*, *iii* and *iv*). This was confirmed by measuring the fibril length in these suspensions of fibrils produced by pipetting (supplemental Fig. 3*B*). After ultracentrifugation, many tiny fibrils were observed in the supernatant of WT fibrils formed in the presence of A30P seeds, whereas few such fibrils were detected in the supernatant of WT fibrils formed in the presence of WT seeds (Fig. 3*A*, *v* and *vi*). Quantitative analysis confirmed that a larger amount of α-synuclein was present in the supernatant of WT fibrils formed in the presence of A30P seeds than in that of WT fibrils formed in the presence of WT seeds (Fig. 3, *B* and *C*). These results suggest that WT fibrils formed in the presence of A30P seeds have the same shedding propensity as A30P fibrils.

Immunochemical Analysis of α-Synuclein Fibrils with Epitope-specific Antibodies—To investigate the structural differences between WT fibrils and A30P fibrils and between WT fibrils formed in the presence of WT seeds and WT fibrils formed in the presence of A30P seeds, we employed a dot blot assay with three epitope-specific antibodies to α-synuclein, syn1–10 (N-terminal region), syn75–91 (NAC region), and syn131–140 (C-terminal region).

As shown in Fig. 4, *G* and *I*, syn131–140 stained both WT and A30P fibrils (fibril seeds) almost equally, whereas syn75–91 (Fig. 4, *E* and *I*) strongly labeled only WT fibrils. syn1–10 (Fig. 4, *C* and *I*) labeled A30P fibrils more strongly than WT fibrils. Similar results were obtained with other independently produced anti-α-synuclein antibodies to the N terminus (number 36, a gift from Dr. Iwatsubo) and anti-NAC antibody (NAC2, a gift form Dr. Jäkälä) (data not shown). These results suggest that the conformation of A30P fibrils is different from that of WT fibrils. Interestingly, dot blot analysis of WT fibrils formed in the presence of A30P seeds showed a pattern of immunore-

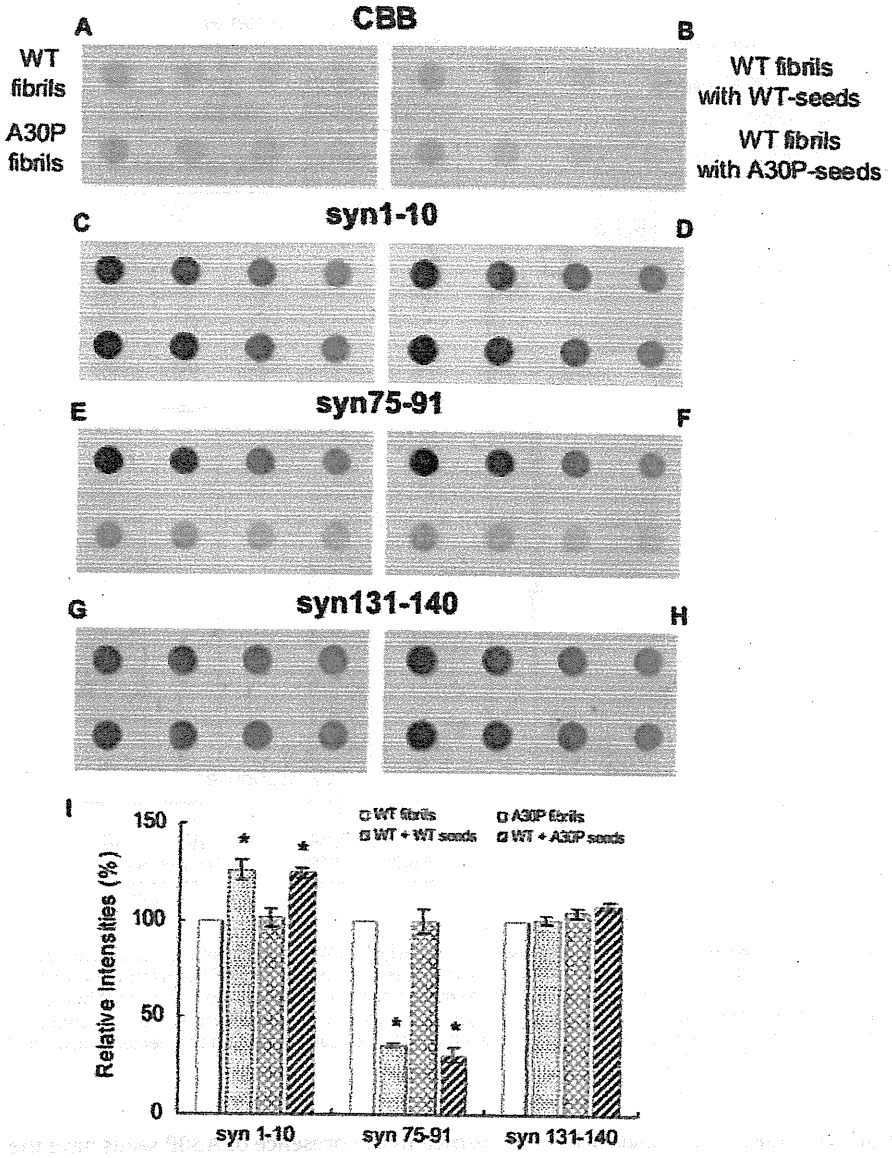

FIGURE 4. **Dot blot analysis of WT fibrils formed in the presence of A30P fibril seeds with epitope-specific antibodies.** Equal amounts of serially diluted WT fibrils, A30P fibrils, WT fibrils formed in the presence of WT seeds, and WT fibrils formed in the presence of A30P seeds were spotted onto polyvinylidene difluoride membrane, stained with CBB (*A* and *B*), or immunodetected with syn1–10 (*C* and *D*), syn75–91 (*E* and *F*), and syn131–140 antibodies (*G* and *H*). For CBB staining and dot blotting with syn74–91, 100, 50, 25, and 12.5 ng of protein were spotted. For immunodetection with syn1–10 and syn131–140, 10, 5, 2.5, and 1.25 ng of protein were spotted. A typical experiment is shown; similar results were obtained in three separate experiments. *I*, quantification of immunoreactivities of WT fibrils, A30P fibrils, and WT fibrils formed in the presence of WT seeds or A30P seeds. The results are expressed as a percentage of immunoreactivity of WT fibrils, taken as 100% (means ± S.E., $n = 3$) (*, $p < 0.01$).

activity similar to that of A30P fibrils (Fig. 4, *D*, *F*, and *I*), whereas WT fibrils formed in the presence of WT seeds showed the same pattern as WT fibrils (Fig. 4, *D*, *F*, and *I*). These results suggest that the WT fibrils formed in the presence of A30P seeds have a similar conformation to that of A30P fibrils. WT or A30P monomer showed very weak immunoreactivities to syn1–10 and syn75–91 (supplemental Fig. 2, *C*, *E*, and *I*). WT fibrils showed comparatively strong immunoreactivities to all three antibodies, whereas A30P fibrils showed a distinct pattern (supplemental Fig. 2, *D*, *F*, and *I*), being labeled strongly with syn1–10 but hardly at all with syn75–91.

Comparison of Protease-resistant Cores of WT and A30P α-Synuclein Fibrils—In order to investigate the structural differences between WT and A30P fibrils and also between WT fibrils formed in the presence of WT seeds and WT fibrils formed in the presence of A30P seeds, we analyzed protease-resistant cores of these fibrils after digestion with trypsin or proteinase K. Amyloid fibrils in neurodegenerative diseases and other types of amyloidosis are known to be highly resistant to many proteases, and the analysis of protease-resistant cores is frequently used for investigating the structures of various amyloid fibrils (34–36).

When monomeric α-synuclein was digested with trypsin or proteinase K, no band was detected (Fig. 5*A*). In contrast, 8–12 kDa core bands remained when the fibrils were treated with trypsin or proteinase K. Trypsin digestion of the fibrils composed of WT afforded two major bands of 10 and ~13 kDa (*black arrowheads*), and a similar band pattern was observed after the digestion of the WT fibrils formed in the presence of the WT seeds. On the other hand, two major bands of 9.5 and ~12.5 kDa (*white arrowheads*) with smaller molecular weights than those of the WT bands were detected after the digestion of A30P fibrils and WT fibrils formed in the presence of A30P seeds (Fig. 5, *B* and *C*). Similarly, digestion of WT fibrils and WT fibrils formed in the presence of WT seeds with proteinase K, a nonspecific protease, showed three major bands of 10–12 kDa (*black arrowheads*), whereas one major band of ~11.5 kDa (*white arrowhead*) was detected after the digestion of A30P fibrils and WT fibrils formed in the presence of A30P seeds (Fig. 5, *B* and *C*). These protein-chemical data strongly suggest that the core structures of A30P fibrils and WT fibrils formed in the presence of A30P seeds are distinct from those of WT fibrils and WT fibrils formed in the presence of WT seeds and further support the immunochemical results described above.

Effect of WT Seeds on Fibrillization of A30P Mutant α-Synuclein—Since WT α-synuclein assembles into fibrils faster than A30P mutant α-synuclein *in vitro* (Fig. 1*A*), WT seeds may be formed earlier than A30P seeds in the brains of

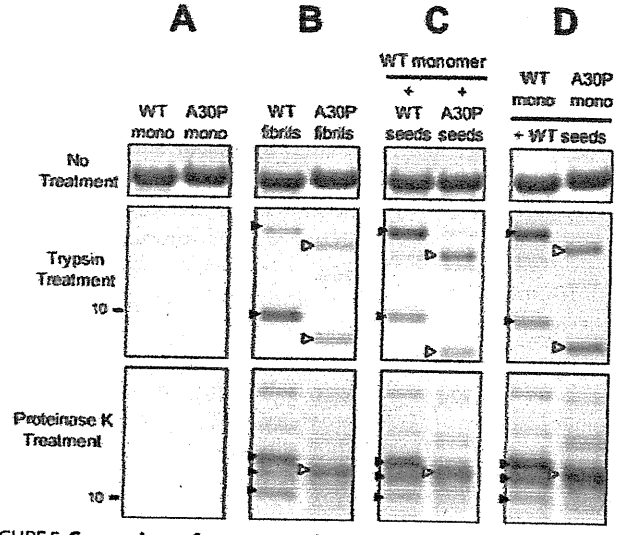

FIGURE 5. **Comparison of protease-resistant cores of WT fibrils, A30P fibrils, WT fibrils formed in the presence of A30P seeds, and A30P fibrils formed in the presence of WT seeds.** Monomeric WT and A30P α-synuclein (*A*), preformed WT and A30P fibrils (*B*), WT fibrils formed in the presence of WT seeds or A30P seeds (*C*), or WT or A30P fibrils formed in the presence of WT seeds (*D*) were treated with trypsin (final 50 μg/ml) or proteinase K (final 2 μg/ml) for 30 min and subjected to SDS-PAGE. Bands were stained with CBB. Note that protease-resistant band patterns of WT fibrils formed with WT seeds are the same as those of WT fibrils (*black arrowheads*), whereas the band patterns of WT fibrils formed with A30P seeds and A30P fibrils formed in the presence of WT seeds are the same as those of A30P seeds (*white arrowheads*). A typical experiment is shown; similar results were obtained in three separate experiments.

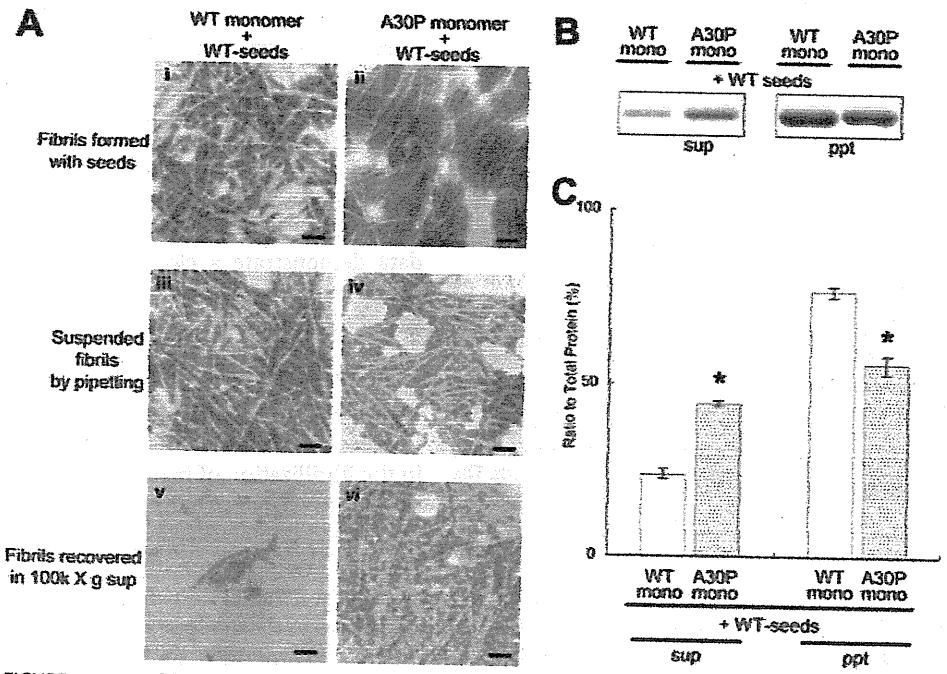

FIGURE 6. **EM and biochemical analyses of A30P fibrils formed in the presence of WT seeds.** *A*, EM analysis of WT fibrils formed in the presence of WT seeds (*i*, *iii*, and *v*) and A30P fibrils formed in the presence of WT seeds (*ii*, *iv*, and *vi*) before and after suspension. Negatively stained WT or A30P fibrils formed in the presence of WT seeds (*i* and *ii*), the fibrils after suspension (*iii* and *iv*), and the fibrils in the supernatants after centrifugation (*v* and *vi*) were observed by electron microscopy. *Scale bar*, 200 nm. *B*, CBB staining of α-synuclein recovered in the supernatants and the pellets after centrifugation of the fibrils. *C*, quantification of α-synuclein recovered in the supernatants and pellets after ultracentrifugation (expressed as a percentage of total α-synuclein, taken as 100%). The results are expressed as means ± S.E. ($n = 3$) (*, $p < 0.01$).

patients with the A30P mutation. We therefore investigated whether A30P mutant α-synuclein can assemble into fibrils in the presence of WT seeds and whether the A30P fibrils formed in the presence of WT seeds show the characteristics of WT fibrils. Nucleation-dependent fibrillization of A30P mutant α-synuclein was observed in the presence of WT seeds. When the A30P fibrils formed in the presence of WT seeds were analyzed by electron microscopy and ultracentrifugation (Fig. 6), the A30P fibrils formed in the presence of WT seeds appeared to be morphologically indistinguishable from the WT fibrils formed in the presence of WT seeds before the preparation of suspensions (Fig. 6*A*, *i* and *ii*). However, after suspension, many tiny fibrils were observed in the A30P fibrils formed in the presence of WT seeds, whereas such short fibrils were hardly detected in the WT fibrils formed in the presence of WT seeds (Fig. 6*A*, *iii* and *iv*). This was confirmed by measuring the length of fibrils in these suspensions prepared by pipetting (supplemental Fig. 3. Many tiny fibrils were observed in the supernatant of A30P fibrils formed in the presence of WT seeds, whereas such tiny fibrils were hardly detected in the supernatant of WT fibrils formed in the presence of WT seeds (Fig. 6*A*, *v* and *vi*). Quantitative analysis of α-synuclein in the supernatants and pellets by SDS-PAGE confirmed the results of EM observation; more α-synuclein was detected in the supernatant of A30P fibrils formed in the presence of WT seeds than in that of WT fibrils formed in the presence of WT seeds (Fig. 6, *B* and *C*). These results indicate that A30P fibrils formed in the presence of WT seeds do not acquire the character of the WT seeds but retain the character of A30P fibrils.

Conformation of A30P Fibrils Formed in the Presence of WT Seeds—To investigate the relationship between the shedding propensity of fibrils and conformation, we analyzed A30P fibrils formed in the presence of WT seeds by dot blot assay using the epitope-specific antibodies (Fig. 7). Surprisingly, A30P fibrils formed in the presence of WT seeds showed the same pattern of immunoreactivity as A30P fibrils, and the pattern was different from that of WT fibrils formed in the presence of WT seeds (Fig. 7, *C*, *D*, *E*, *F*, and *I*). Similar results were obtained with number 36 and NAC2 antibodies (data not shown).

To further investigate the structural differences between WT fibrils formed in the presence of WT seeds and A30P fibrils formed in the presence of WT seeds, the protease-resistant cores of the fibrils were analyzed. As shown in Fig. 5, *B* and *D*, the band patterns of the trypsin- and proteinase K-resistant cores of A30P fibrils formed in the presence

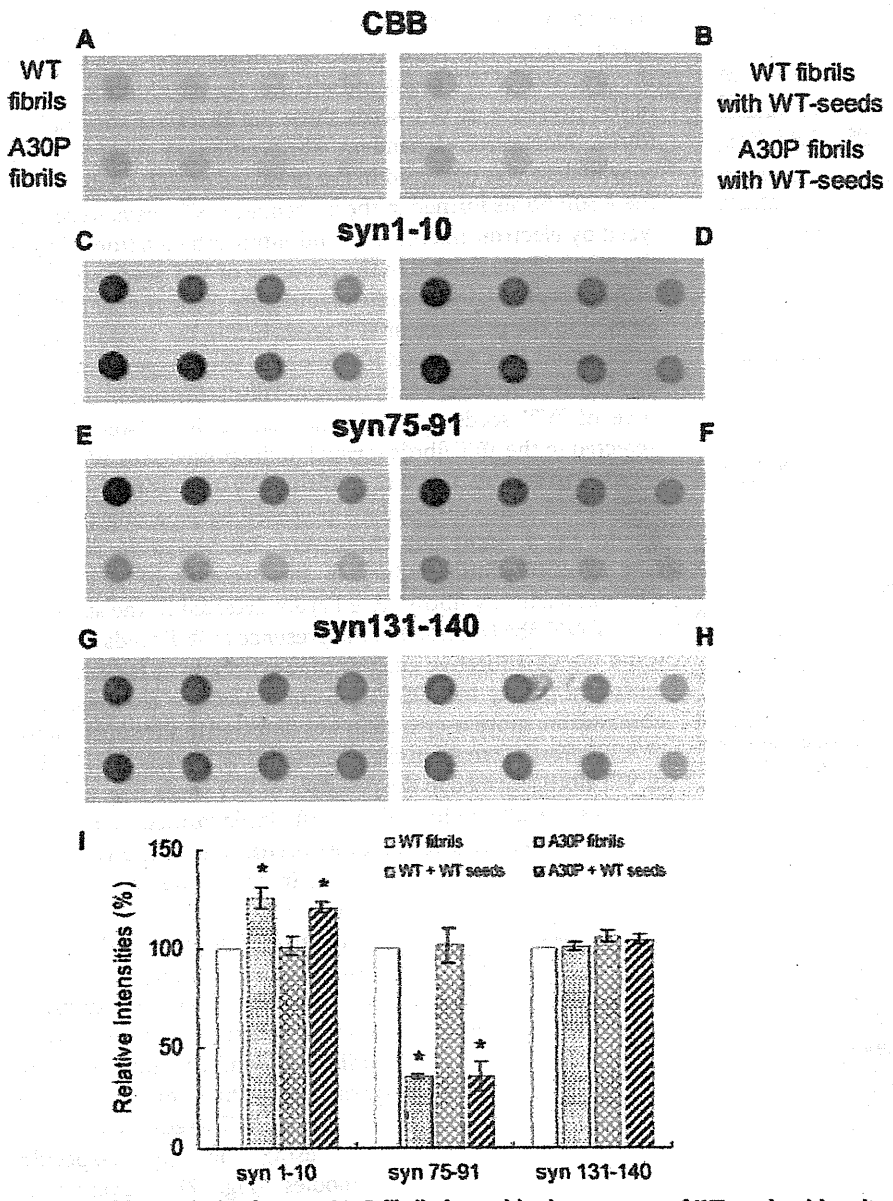

FIGURE 7. **Dot blot analysis of WT or A30P fibrils formed in the presence of WT seeds with epitope-specific antibodies.** Equal amounts of WT and A30P fibrils, WT fibrils formed in the presence of WT seeds, and A30P fibrils formed in the presence of WT seeds were spotted on polyvinylidene difluoride membrane and stained with CBB (*A* and *B*) or immunodetected with syn1–10 (*C* and *D*), syn75–91 (*E* and *F*), or syn131–140 antibodies (*G* and *H*). For CBB staining and dot blotting with syn74–91, 100, 50, 25, and 12.5 ng of protein were spotted. For immunodetection with syn1–10 and syn131–140, 10, 5, 2.5, and 1.25 ng of protein were spotted. A typical experiment is shown; similar results were obtained in three separate experiments. *I*, quantification of immunoreactivities of WT fibrils, A30P fibrils, and WT or A30P fibrils formed in the presence of WT seeds. The results are expressed as a percentage of immunoreactivity of WT fibrils, taken as 100% (means ± S.E., $n = 3$) (*, $p < 0.01$).

of WT seeds were the same as those of A30P fibrils (*white arrowheads*) and distinct from those of WT fibrils and WT fibrils formed with WT seeds (*black arrowheads*). These results strongly support the view that A30P fibrils formed in the presence of WT seeds do not acquire the conformation of the WT seeds but retain the conformation of A30P fibrils.

Cytotoxicities of WT and Mutant α-Synuclein Fibrils—To investigate the relationship between the shedding propensity of fibrils and the cytotoxicity, SH-SY5Y cells were treated with WT or mutant fibrils (suspended by pipetting or sonication), and the cytotoxicity was determined by an MTT reduction assay, as has been used widely. As shown in Fig. 8*A*, all fibrils composed of WT or mutant α-synuclein showed a significant reduction of MTT ($p < 0.01$), whereas no toxicity was detected with monomeric WT or mutant α-synuclein. Interestingly, A30P fibrils showed a stronger effect than WT fibrils or the other mutant fibrils, suggesting a link between shedding propensity and cytotoxicity. When cells were treated with sonicated fibrils, which were fragmented homogeneously to short fibrils (data not shown), the cytotoxicity was significantly enhanced ($p < 0.01$), although the increase was small in the case of the E46K mutant (Fig. 8*A*). These results indicate that large numbers of short fibrils are more toxic than small numbers of long fibrils. It is possible that short fibrils can interact with cell membranes more easily than long fibrils. The cytotoxicities of WT fibrils formed in the presence of A30P seeds and A30P fibrils formed in the presence of WT seeds were also analyzed by MTT assay (Fig. 8*B*). These fibrils with increased shedding propensity showed stronger cytotoxicity than WT fibrils formed in the presence of WT seeds, and sonication enhanced the toxic effects of these fibrils. These data demonstrate a close correlation between the shedding propensity of fibrils and the cytotoxicity.

DISCUSSION

Nucleation-dependent aggregation has been reported to play a role in the fibrillization of many amyloidogenic proteins, including Aβ protein, β2-microglobulin, and apoA-II (37–39). Assembly of α-synuclein into fibrils has also been shown to be a nucleation-dependent process (22). In this study, we have extensively investigated the nucleation-dependent assembly of WT and mutant α-synuclein into fibrils, the shedding properties of these fibrils, and the conformational differences between WT and A30P fibrils and between these fibrils formed in the presence of different seeds. The addition of A30P seeds to WT monomer promoted the fibrillization of WT α-synuclein, indicating that A30P fibrils have a cross-seeding effect on WT α-synuclein. Surprisingly, A30P seeds promoted the fibrillization of WT

Effect of A30P Mutation on Fibrillization of α-Synuclein

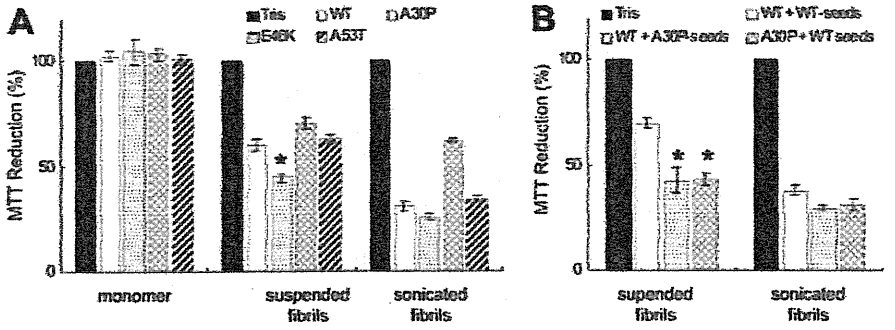

FIGURE 8. **Cytotoxicities of WT and mutant α-synuclein fibrils.** *A*, SH-SY5Y cells were treated with monomeric WT or mutant α-synuclein, suspended fibrils, or sonicated fibrils, and cellular damage was detected by an MTT reduction assay. Significant reduction of MTT was detected in cells treated with WT and mutant fibrils ($p > 0.01$), whereas no toxicity was detected in the case of monomeric α-synuclein. *B*, cytotoxic effects of WT fibrils formed in the presence of WT seeds or A30P seeds and A30P fibrils formed in the presence of WT seeds (suspended or sonicated). The results are presented as percentage MTT reduction, with the values obtained upon the addition of 30 mM Tris-HCl, pH 7.5, taken as 100%. The results are expressed as means ± S.E. ($n = 3$) (*, $p < 0.01$).

faster than did WT, E46K, and A53T seeds. In contrast, the seeding effect of A53T seeds on WT α-synuclein was similar to that of WT seeds, and that of E46K seeds was much smaller. EM and ultracentrifugation studies revealed that the strong seeding effect of A30P was due to the enhanced shedding propensity of A30P fibrils. A similar effect of amyloid fibrils has been found in studies of yeast prion protein (Sup35) (40). Sup35 N-terminal residues 1–254 (SupNM) assembled into amyloid fibrils with different conformations, Sc4 or Sc37, upon incubation at 4 or 37 °C, respectively. Sc4 had a higher fragility than Sc37, and only Sc4 amyloid had high infectivity and seeding efficacy for fibrillization of Sup35 monomer. Furthermore, it has been reported that pathological prion protein can be detected sensitively by cyclic amplification of protein misfolding with sonication (41). These reports demonstrate that fragmentation or shedding of amyloid fibrils can accelerate fibrillization and result in high infectivity and are therefore consistent with our findings here. Substitution of alanine to proline at residue 30 may have a significant effect on the conformation of α-synuclein monomer and assembled fibrils. Proline introduces a bend in the peptide chain, abolishing α-helix structure and disrupting β-sheets. It has been shown that in the A30P mutant, a region of helical structure (residues 18–31) that exists in WT is abolished, formation of β-sheet-rich mature fibril structure is retarded, and the polypeptide backbone stiffness (segment length of about 5 residues) is increased (42, 43). Since the A30P mutation exists in the vicinity of the N terminus of the fibril core (residues 31–109) (34), it is reasonable to speculate that the proline residue would affect both fibrillization and the conformation of the fibrils.

To investigate whether the structural and biochemical features of A30P fibrils can be transmitted to WT fibrils formed in the presence of A30P seeds, we analyzed the fibrils by electron microscopy, ultracentrifugation, dot blot assay, and protease-resistant core analysis. The results clearly demonstrated that the unique features of A30P fibrils were transmitted to WT fibrils grown in the presence of A30P seeds. Transmission of structures and features of fibrils has been reported in other amyloidogenic proteins, such as prion proteins and Aβ. When amyloid fibrils of Syrian hamster prion protein were added to mouse prion protein, the mouse prion protein formed Syrian hamster-type amyloid fibrils but not mouse-type fibrils (44). A similar effect has been seen with yeast prion protein and Aβ (45, 46).

In this study, we have employed a novel method using epitope-specific antibodies of α-synuclein to detect structural difference between WT fibrils and A30P fibrils (Fig. 4). Dot blot analysis also revealed the presence of conformational differences between α-synuclein monomer and the fibrils (supplemental Fig. 2). WT fibrils were recognized very strongly by antibodies to the N-terminal region and NAC region, whereas the monomers were only weakly recognized by these antibodies. Since the N-terminal region and C-terminal region of α-synuclein show intramolecular long range interactions (15), it is reasonable that antibodies to the N terminus and NAC region cannot access the epitopes in the monomer. The results also suggest that the N-terminal and NAC regions of α-synuclein are both exposed at the surface in the fibrils (supplemental Fig. 2, *D*, *F*, and *I*). In A30P, however, the NAC region is buried in the fibrils (supplemental Fig. 2, *F* and *I*), probably because the bent N terminus masks the NAC region and blocks recognition by the corresponding antibody. Recent single molecule studies *in vitro* have shown that under conditions similar to physiological, α-synuclein exists as three distinct conformers that are characterized by long distance weak interactions, random coil structure, and β-like structure and that the relative abundance of β-like conformer is increased in A30P mutant (47). This is in good agreement with our observations by dot blot assay of WT and A30P monomeric α-synuclein with epitope-specific antibodies.

In this study, fibrillization of the A30P monomer was slower than that of WT, but the seeding effect of A30P on the fibrillization was stronger than that of WT. This reciprocal effect of A30P monomer and the fibrils may explain the different results in the aggregation experiments.

In the EM and biochemical analyses of seeds, we found that small fibril fragments are recovered in the supernatant of A30P fibrils and that these fragments act as seeds. This is surprising, because the supernatant after ultracentrifugation is normally referred to as the soluble fraction in biochemistry. Some reports have suggested the presence of nonfibrillar soluble oligomers or abnormal species in the soluble fractions of diseased brains. It is possible that such soluble oligomers or abnormal species may correspond to small fibrils or fragments.

In this *in vitro* study, we found an important effect of A30P mutation, which may provide a clue for understanding the mechanism of early onset in patients harboring the A30P mutation. Our schematic models of nucleation-dependent fibrillization are shown in Fig. 9. WT fibrils formed in the presence of A30P seeds possess the structural and functional characteristics of A30P fibrils (Fig. 9*A*), whereas A30P fibrils formed in the presence of WT seeds do not acquire the character of the WT seeds but retain the features of A30P fibrils (Fig. 9*B*). Recent

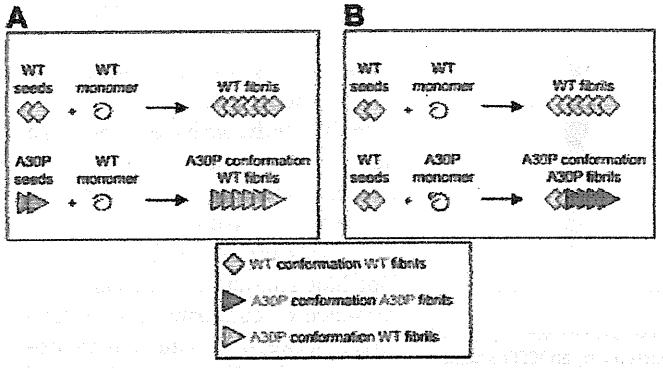

FIGURE 9. **Schematic illustration of proposed nucleation-dependent fibrillization of WT and A30P mutant α-synuclein.** *A*, fibrillization of WT α-synuclein in the presence of WT seeds or A30P seeds. When WT seeds are added to WT monomer, WT fibrils are formed (*top*). When A30P seeds are added to WT monomer, WT fibrils with the character and conformation of A30P fibrils are formed (*bottom*). *B*, fibrillization of A30P α-synuclein in the presence of WT seeds. When WT seeds are added to A30P monomer, A30P fibrils with the usual A30P fibril conformation are formed.

immunohistochemical analyses of the brains of PD patients who underwent transplantation have shown that α-synuclein lesions can propagate from host to grafted cells (48, 49). Thus, fibrillization of α-synuclein in the brains of patients with A30P mutation may also be faster than in normal brains. We would like to investigate this possibility in the future.

REFERENCES

1. Spillantini, M. G., Crowther, R. A., Jakes, R., Hasegawa, M., and Goedert, M. (1998) *Proc. Natl. Acad. Sci. U. S. A.* **95,** 6469–6473
2. Baba, M., Nakajo, S., Tu, P. H., Tomita, T., Nakaya, K., Lee, V. M., Trojanowski, J. Q., and Iwatsubo, T. (1998) *Am. J. Pathol.* **152,** 879–884
3. Fujiwara, H., Hasegawa, M., Dohmae, N., Kawashima, A., Masliah, E., Goldberg, M. S., Shen, J., Takio, K., and Iwatsubo, T. (2002) *Nat. Cell Biol.* **4,** 160–164
4. Polymeropoulos, M. H., Lavedan, C., Leroy, E., Ide, S. E., Dehejia, A., Dutra, A., Pike, B., Root, H., Rubenstein, J., Boyer, R., Stenroos, E. S., Chandrasekharappa, S., Athanassiadou, A., Papapetropoulos, T., Johnson, W. G., Lazzarini, A. M., Duvoisin, R. C., Di Iorio, G., Golbe, L. I., and Nussbaum, R. L. (1997) *Science* **276,** 2045–2047
5. Kruger, R., Kuhn, W., Muller, T., Woitalla, D., Graeber, M., Kosel, S., Przuntek, H., Epplen, J. T., Schols, L., and Riess, O. (1998) *Nat. Genet.* **18,** 106–108
6. Zarranz, J. J., Alegre, J., Gomez-Esteban, J. C., Lezcano, E., Ros, R., Ampuero, I., Vidal, L., Hoenicka, J., Rodriguez, O., Atares, B., Llorens, V., Gomez Tortosa, E., del Ser, T., Munoz, D. G., and de Yebenes, J. G. (2004) *Ann. Neurol.* **55,** 164–173
7. Singleton, A. B., Farrer, M., Johnson, J., Singleton, A., Hague, S., Kachergus, J., Hulihan, M., Peuralinna, T., Dutra, A., Nussbaum, R., Lincoln, S., Crawley, A., Hanson, M., Maraganore, D., Adler, C., Cookson, M. R., Muenter, M., Baptista, M., Miller, D., Blancato, J., Hardy, J., and Gwinn-Hardy, K. (2003) *Science* **302,** 841
8. Farrer, M., Kachergus, J., Forno, L., Lincoln, S., Wang, D. S., Hulihan, M., Maraganore, D., Gwinn-Hardy, K., Wszolek, Z., Dickson, D., and Langston, J. W. (2004) *Ann. Neurol.* **55,** 174–179
9. Chartier-Harlin, M. C., Kachergus, J., Roumier, C., Mouroux, V., Douay, X., Lincoln, S., Levecque, C., Larvor, L., Andrieux, J., Hulihan, M., Waucquier, N., Defebvre, L., Amouyel, P., Farrer, M., and Destee, A. (2004) *Lancet* **364,** 1167–1169
10. Ibanez, P., Bonnet, A. M., Debarges, B., Lohmann, E., Tison, F., Pollak, P., Agid, Y., Durr, A., and Brice, A. (2004) *Lancet* **364,** 1169–1171
11. Nishioka, K., Hayashi, S., Farrer, M. J., Singleton, A. B., Yoshino, H., Imai, H., Kitami, T., Sato, K., Kuroda, R., Tomiyama, H., Mizoguchi, K., Murata, M., Toda, T., Imoto, I., Inazawa, J., Mizuno, Y., and Hattori, N. (2006) *Ann. Neurol.* **59,** 298–309
12. Fuchs, J., Nilsson, C., Kachergus, J., Munz, M., Larsson, E. M., Schule, B., Langston, J. W., Middleton, F. A., Ross, O. A., Hulihan, M., Gasser, T., and Farrer, M. J. (2007) *Neurology* **68,** 916–922
13. Davidson, W. S., Jonas, A., Clayton, D. F., and George, J. M. (1998) *J. Biol. Chem.* **273,** 9443–9449
14. Uversky, V. N., Li, J., and Fink, A. L. (2001) *J. Biol. Chem.* **276,** 10737–10744
15. Bertoncini, C. W., Jung, Y. S., Fernandez, C. O., Hoyer, W., Griesinger, C., Jovin, T. M., and Zweckstetter, M. (2005) *Proc. Natl. Acad. Sci. U. S. A.* **102,** 1430–1435
16. Spillantini, M. G., Schmidt, M. L., Lee, V. M., Trojanowski, J. Q., Jakes, R., and Goedert, M. (1997) *Nature* **388,** 839–840
17. Serpell, L. C., Berriman, J., Jakes, R., Goedert, M., and Crowther, R. A. (2000) *Proc. Natl. Acad. Sci. U. S. A.* **97,** 4897–4902
18. Crowther, R. A., Daniel, S. E., and Goedert, M. (2000) *Neurosci. Lett.* **292,** 128–130
19. Biere, A. L., Wood, S. J., Wypych, J., Steavenson, S., Jiang, Y., Anafi, D., Jacobsen, F. W., Jarosinski, M. A., Wu, G. M., Louis, J. C., Martin, F., Narhi, L. O., and Citron, M. (2000) *J. Biol. Chem.* **275,** 34574–34579
20. Giasson, B. I., Murray, I. V., Trojanowski, J. Q., and Lee, V. M. (2001) *J. Biol. Chem.* **276,** 2380–2386
21. Conway, K. A., Harper, J. D., and Lansbury, P. T. (1998) *Nat. Med.* **4,** 1318–1320
22. Narhi, L., Wood, S. J., Steavenson, S., Jiang, Y., Wu, G. M., Anafi, D., Kaufman, S. A., Martin, F., Sitney, K., Denis, P., Louis, J. C., Wypych, J., Biere, A. L., and Citron, M. (1999) *J. Biol. Chem.* **274,** 9843–9846
23. Conway, K. A., Lee, S. J., Rochet, J. C., Ding, T. T., Williamson, R. E., and Lansbury, P. T., Jr. (2000) *Proc. Natl. Acad. Sci. U. S. A.* **97,** 571–576
24. Conway, K. A., Harper, J. D., and Lansbury, P. T., Jr. (2000) *Biochemistry* **39,** 2552–2563
25. Greenbaum, E. A., Graves, C. L., Mishizen-Eberz, A. J., Lupoli, M. A., Lynch, D. R., Englander, S. W., Axelsen, P. H., and Giasson, B. I. (2005) *J. Biol. Chem.* **280,** 7800–7807
26. Goldberg, M. S., and Lansbury, P. T., Jr. (2000) *Nat. Cell Biol.* **2,** E115–E119
27. Volles, M. J., and Lansbury, P. T., Jr. (2002) *Biochemistry* **41,** 4595–4602
28. Jensen, P. H., Nielsen, M. S., Jakes, R., Dotti, C. G., and Goedert, M. (1998) *J. Biol. Chem.* **273,** 26292–26294
29. Jo, E., Fuller, N., Rand, R. P., St George-Hyslop, P., and Fraser, P. E. (2002) *J. Mol. Biol.* **315,** 799–807
30. Wood, S. J., Wypych, J., Steavenson, S., Louis, J. C., Citron, M., and Biere, A. L. (1999) *J. Biol. Chem.* **274,** 19509–19512
31. Masuda, M., Dohmae, N., Nonaka, T., Oikawa, T., Hisanaga, S., Goedert, M., and Hasegawa, M. (2006) *FEBS Lett.* **580,** 1775–1779
32. Taniguchi, S., Suzuki, N., Masuda, M., Hisanaga, S., Iwatsubo, T., Goedert, M., and Hasegawa, M. (2005) *J. Biol. Chem.* **280,** 7614–7623
33. Masuda, M., Suzuki, N., Taniguchi, S., Oikawa, T., Nonaka, T., Iwatsubo, T., Hisanaga, S., Goedert, M., and Hasegawa, M. (2006) *Biochemistry* **45,** 6085–6094
34. Miake, H., Mizusawa, H., Iwatsubo, T., and Hasegawa, M. (2002) *J. Biol. Chem.* **277,** 19213–19219
35. Aoyagi, H., Hasegawa, M., and Tamaoka, A. (2007) *J. Biol. Chem.* **282,** 20309–20318
36. Raymond, G. J., Hope, J., Kocisko, D. A., Priola, S. A., Raymond, L. D., Bossers, A., Ironside, J., Will, R. G., Chen, S. G., Petersen, R. B., Gambetti, P., Rubenstein, R., Smits, M. A., Lansbury, P. T., Jr., and Caughey, B. (1997) *Nature* **388,** 285–288
37. Naiki, H., Higuchi, K., Nakakuki, K., and Takeda, T. (1991) *Lab. Invest.* **65,** 104–110
38. Jarrett, J. T., and Lansbury, P. T., Jr. (1993) *Cell* **73,** 1055–1058
39. Naiki, H., and Gejyo, F. (1999) *Methods Enzymol.* **309,** 305–318
40. Tanaka, M., Collins, S. R., Toyama, B. H., and Weissman, J. S. (2006) *Nature* **442,** 585–589
41. Saborio, G. P., Permanne, B., and Soto, C. (2001) *Nature* **411,** 810–813
42. Lee, J. C., Langen, R., Hummel, P. A., Gray, H. B., and Winkler, J. R. (2004)

Proc. Natl. Acad. Sci. U. S. A. **101,** 16466–16471
43. Bussell, R., Jr., and Eliezer, D. (2001) *J. Biol. Chem.* **276,** 45996–46003
44. Jones, E. M., and Surewicz, W. K. (2005) *Cell* **121,** 63–72
45. Petkova, A. T., Leapman, R. D., Guo, Z., Yau, W. M., Mattson, M. P., and Tycko, R. (2005) *Science* **307,** 262–265
46. Tanaka, M., Chien, P., Yonekura, K., and Weissman, J. S. (2005) *Cell* **121,** 49–62
47. Sandal, M., Valle, F., Tessari, I., Mammi, S., Bergantino, E., Musiani, F., Brucale, M., Bubacco, L., and Samorì, B. (2008) *PLoS Biol.* **6,** e6
48. Li, J. Y., Englund, E., Holton, J. L., Soulet, D., Hagell, P., Lees, A. J., Lashley, T., Quinn, N. P., Rehncrona, S., Bjorklund, A., Widner, H., Revesz, T., Lindvall, O., and Brundin, P. (2008) *Nat. Med.* **14,** 501–503
49. Kordower, J. H., Chu, Y., Hauser, R. A., Freeman, T. B., and Olanow, C. W. (2008) *Nat. Med.* **14,** 504–506

FEBS Letters 583 (2009) 787–791

ELSEVIER

FEBS Letters

journal homepage: www.FEBSLetters.org

Inhibition of α-synuclein fibril assembly by small molecules: Analysis using epitope-specific antibodies

Masami Masuda [a,b], Masato Hasegawa [a,*], Takashi Nonaka [a], Takayuki Oikawa [a,b], Motokuni Yonetani [a,b], Yoshiki Yamaguchi [c], Koichi Kato [c], Shin-ichi Hisanaga [b], Michel Goedert [d,*]

[a] *Department of Molecular Neurobiology, Tokyo Institute of Psychiatry, 2-1-8 Kamikitazawa, Setagaya-ku, Tokyo 156-8585, Japan*
[b] *Molecular Neuroscience Laboratory, Graduate School of Science, Tokyo Metropolitan University, 1-1 Minami-Osawa, Hachioji-shi Tokyo 192-0397, Japan*
[c] *Department of Structural Biology and Biomolecular Engineering, Graduate School of Pharmaceutical Science, Nagoya City University, 3-1 Tanabe-dori, Mizuho-ku, Nagoya 467-8603, Japan*
[d] *MRC Laboratory of Molecular Biology, Hills Road, Cambridge CB2 0QH, UK*

FEBS Letters 583 (2009) 787–791

journal homepage: www.FEBSLetters.org

Inhibition of α-synuclein fibril assembly by small molecules: Analysis using epitope-specific antibodies

Masami Masuda [a,b], Masato Hasegawa [a,*], Takashi Nonaka [a], Takayuki Oikawa [a,b], Motokuni Yonetani [a,b], Yoshiki Yamaguchi [c], Koichi Kato [c], Shin-ichi Hisanaga [b], Michel Goedert [d,*]

[a] Department of Molecular Neurobiology, Tokyo Institute of Psychiatry, 2-1-8 Kamikitazawa, Setagaya-ku, Tokyo 156-8585, Japan
[b] Molecular Neuroscience Laboratory, Graduate School of Science, Tokyo Metropolitan University, 1-1 Minami-Osawa, Hachioji-shi Tokyo 192-0397, Japan
[c] Department of Structural Biology and Biomolecular Engineering, Graduate School of Pharmaceutical Science, Nagoya City University, 3-1 Tanabe-dori, Mizuho-ku, Nagoya 467-8603, Japan
[d] MRC Laboratory of Molecular Biology, Hills Road, Cambridge CB2 0QH, UK

ARTICLE INFO

Article history:
Received 8 December 2008
Revised 3 January 2009
Accepted 20 January 2009
Available online 4 February 2009

Edited by Jesus Avila

Keywords:
Tau
Amyloid
Polyphenol
Oligomer
Conformation
Aggregation

ABSTRACT

The conversion of soluble peptides and proteins into amyloid fibrils and/or intermediate oligomers is believed to be the central event in the pathogenesis of most human neurodegenerative diseases. Existing treatments are at best symptomatic. Accordingly, small molecule inhibitors of amyloid fibril formation and their mechanisms are of great interest. Here we report that the conformational changes undergone by α -synuclein as it assembles into amyloid fibrils can be detected by epitope-specific antibodies. We show that the conformations of polyphenol-bound α-synuclein monomers and dimers differ from those of unbound monomers and resemble amyloid fibrils. This strongly suggests that small molecule inhibitors bind and stabilize intermediates of amyloid fibril formation, consistent with the view that inhibitor-bound molecular species are on-pathway intermediates.

1. Introduction

The conversion of a small number of soluble peptides and proteins into amyloid fibrils and/or intermediate oligomers is believed to be the central event in the pathogenesis of most neurodegenerative diseases. Three proteins, β-amyloid, tau and α-synuclein, make up the abnormal deposits in the vast majority of disease cases [1,2]. Many current therapeutic strategies are aimed at inhibiting filament formation and at promoting filament clearance. In recent years, a number of compounds has been identified that prevent amyloid fibril formation in vitro [3–10]. In the absence of effective therapies for neurodegenerative diseases, it is important to understand the mechanisms of action of these compounds.

We previously reported that non-toxic, SDS-stable dimers and oligomers of tau and α-synuclein formed in the presence of inhibitory compounds and that their formation closely correlated with the inhibition of fibril formation [8,9]. This suggests that small molecule inhibitors stabilize non-toxic, on-pathway intermediates. Based on these observations, we presented a model for the inhibition of tau, α-synuclein and Aβ aggregation by small molecules. Ehrnhoefer et al. recently presented a different model for the inhibition of fibril formation of α-synuclein and Aβ by the small molecule inhibitor (−)-epigallocatechin-3-gallate (EGCG) [11]. They reported that EGCG inhibited the assembly of α-synuclein and Aβ by binding to natively unfolded protein monomers, preventing their conversion into toxic on-pathway aggregation intermediates. Instead, α-synuclein and Aβ formed unstructured, non-toxic oligomers that were said to be off-pathway.

In this study, we used 10 epitope-specific antibodies of α-synuclein spanning the whole of α-synuclein and investigated their reactivities with monomeric α-synuclein and with α-synuclein fibrils. Some antibodies detected conformational changes that distinguished monomers from fibrils. These antibodies were then used to detect conformational changes in polyphenol-stabilized monomers and dimers of α-synuclein. Importantly, SDS-stable, polyphenol-stabilized monomers and dimers showed an intermediate reactivity between that of monomers and fibrils. These findings indicate that inhibitory compounds bind and stabilize on-pathway intermediates of amyloid fibril formation.

* Corresponding authors. Fax: +81 3 3329 8035.
E-mail addresses: masato@prit.go.jp (M. Hasegawa), mg@mrc-lmb.cam.ac.uk (M. Goedert).

0014-5793/$34.00
doi:10.1016/j.febslet.2009.01.037

2. Materials and methods

2.1. Antibodies

Polyclonal antibodies were raised against synthetic peptides corresponding to residues 1–10, 11–20, 21–30, 31–40, 41–50, 51–60, 61–70, 75–91 and 131–140 of human α-synuclein, with Cys at the C-terminus or the N-terminus (Greiner Bio-One Co. Ltd.) (Table 1). The peptides were conjugated to *m*-maleimidobenzoyl-*N*-hydrosuccinimide ester-activated keyhole limpet hemocyanin (KLH). The KLH-peptide complex (1 mg of each immunogen) emulsified in Freund's complete adjuvant was injected subcutaneously into a New Zealand White rabbit, followed by 5 weekly subcutaneous injections of 150 μg KLH-peptide complex emulsified in Freund's incomplete adjuvant, starting 3 weeks after the first immunization. Antibody Syn259, which recognizes residues 104–119 of α-synuclein, was kindly provided by Dr. S. Nakajo.

2.2. Expression and purification of α-synuclein

Human α-synuclein was expressed in *E. coli* BL21 (DE3) cells, as described [9]. To avoid the production of α-synuclein dimers induced by misexpression of cysteine-containing α-synuclein, the Y136-TAT construct was used [12]. α-Synuclein was purified by boiling, Q-Sepharose ion exchange chromatography and ammonium sulfate precipitation, followed by dialysis against 30 mM Tris–HCl, pH 7.5, and the determination of protein concentrations, as described [9].

2.3. Preparation of α-synuclein fibrils and inhibitor-bound monomers and dimers

Purified α-synuclein (7 mg/ml) was incubated at 37 °C in a shaking incubator (200 rpm) in 30 mM Tris–HCl, pH 7.5, containing 0.1% NaN_3, for 72 h. Fibrils were pelleted by spinning the assembly mixtures at 113 000×*g* for 20 min. To prepare SDS-stable, inhibitor-bound monomers and dimers, the polyphenol exifone was used in most experiments [9]. Similar results were obtained with dopamine and gossypetin, two previously described inhibitory compounds [4,9]. Exifone-bound α-synuclein monomers (Exi-monomer) and dimers (Exi-dimer) were prepared by gel filtration, as described [9]. Briefly, α-synuclein (7 mg/ml) was incubated in the presence of 2 mM inhibitory compound at 37 °C for 72 h in 30 mM Tris-HCl containing 0.1% sodium azide, and centrifuged at 113 000×*g* for 20 min. The supernatants were loaded onto a Superdex 200 gel filtration column (1 × 30 cm), eluted in 10 mM Tris–HCl, pH 7.5, containing 150 mM NaCl, and monitored at 214 nm. Fractionated samples were analyzed by SDS–PAGE and immunoblotting. Protein concentrations were determined as described [9].

Table 1
Antigen peptides for immunization of rabbits.

Name of antibodies	AA residues	Antigen peptide
Syn1-10	1–10	MDVFMKGLSKC
Syn11-20	11–20	AKEGVVAAAEC
Syn21-30	21–30	KTKQGVAEAAC
Syn31-40	31–40	GKTKEGVLYVC
Syn41-50	41–50	GSKTKEGVVHC
Syn51-60	51–60	GVATVAEKTKC
Syn61-70	61–70	EQVTNVGGAVC
Syn75-91	75–91	CTAVAQKTVEGAGSIAAA
Syn131-140	131–140	CEGYQDYEPEA

2.4. ELISA and dot blot assay

For the ELISA, peptide immunogens, α-synuclein monomers and fibrils, as well as Exi-monomers and dimers (0.5–1.0 μg/well in 50 mM Tris–HCl, pH 8.8) were coated onto microtitre plates (SUMILON) at 4 °C for 16 h. The plates were blocked with 10% fetal bovine serum (FBS) in PBS, incubated with the first antibody diluted in 10% FBS/PBS at room temperature for 1.5 h, followed by incubation with HRP-goat anti-rabbit IgG (Bio-Rad) at 1:1000 dilution, and reacted with the substrate, 0.4 mg/ml *o*-phenylendiamine, in citrate buffer (24 mM citric acid, 51 mM Na_2HPO_4). The absorbance at 490 nm was measured using Plate Chameleon (HIDEX). For the dot blot assay, 100 ng α-synuclein was spotted onto a PVDF membrane by using a dot blot apparatus (Bio-Rad). Membranes were stained with Coomassie Brilliant Blue or blocked with 3% gelatin/PBS and incubated overnight at room temperature with anti-α-synuclein antibodies in 10% FBS/PBS. Immunoreactivity was detected with avidin-biotin (Vector Laboratories) and developed using NiCl-enhanced diaminobenzidine. The rate of reactivity was quantified by scanning densitometry and expressed relative to the density of α-synuclein fibrils (taken as 100%).

3. Results

3.1. Antibody specificities

In order to detect conformational changes in α-synuclein, antibodies were raised against nine peptides (corresponding to residues 1–10, 11–20, 21–30, 31–40, 41–50, 51–60, 61–70, 75–91 and 131–140) (Table 1). The specificities of the antibodies were analyzed by ELISA. The peptides used as immunogens were coated on a plate and probed with each antibody. As shown in Fig. 1, each antibody reacted strongly with the appropriate peptide, but hardly with the other peptides. Antibody Syn41–50 was an exception, in that it weakly recognized peptides 11–20 and 31–40, in addition to recognizing peptide 41–50 very strongly.

3.2. Analysis of conformational changes in α-synuclein using epitope-specific antibodies

We investigated the reactivity of monomeric α-synuclein and of α-synuclein fibrils by dot blot assay using the nine antibodies described above and antibody Syn259 whose epitope corresponds to residues 104–119 of α-synuclein. Monomeric α-synuclein was strongly detected by antibodies to the C-terminal region (Syn259 and Syn131–140), but not by antibodies to the N-terminal or middle region (Fig. 2). This is in good agreement with previous reports showing that the C-terminal region of α-synuclein is unfolded and shields the N-terminal and central regions by way of long-range intramolecular interactions [13,14]. In contrast, α-synuclein fibrils were strongly immunoreactive with all antibodies (Fig. 2), indicating that the relevant epitopes were accessible. This is also consistent with current knowledge of the location of individual β-strands and their connecting loops in the structure of the α -synuclein fibril [15,16]. These results indicate that conformational changes undergone by α-synuclein as it assembles into fibrils can be detected immunochemically. We next analyzed the conformations of exifone-stabilized monomers and dimers of α-synuclein, following their separation by gel filtration chromatography (Supplementary Fig.). SDS-stable dimers formed in the presence of exifone were recognized by antibodies specific for Syn1–10, Syn11–20, Syn21–30, Syn31–40 and Syn41–50 (Fig. 2). They were less well recognized by antibodies specific for Syn51–60, Syn61–70 and Syn75–91. The antibody recognition patterns of SDS-stable monomers formed in the presence of exifone were intermediate between

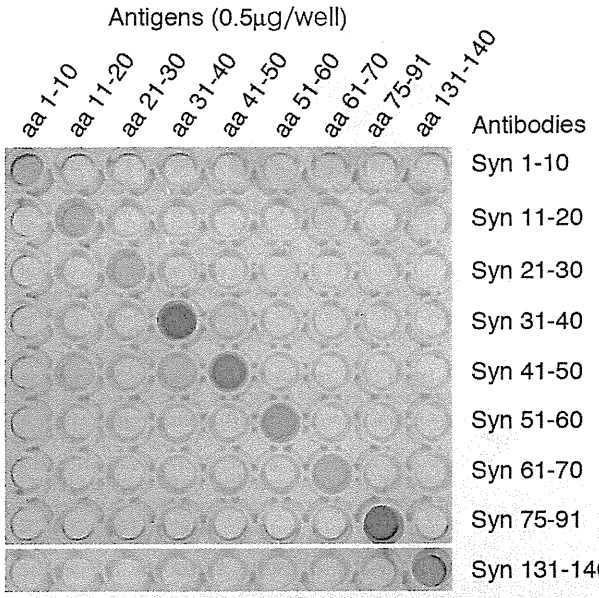

Fig. 1. Specificities of anti-peptide antibodies spanning the whole of α-synuclein determined by ELISA. Synthetic peptides (0.5 µg/well) were coated on a 96-well microtitre plate for 16 h at 4 °C and each of the 9 peptides was probed with each of the 9 antisera.

those of untreated monomers and polyphenol-stabilized dimers (Fig. 2). All antibodies gave similar results by ELISA (data not shown).

4. Discussion

We show here that the conformational changes undergone by α-synuclein during the conversion from monomers to amyloid fibrils can be detected by epitope-specific antibodies. Antibodies to the C-terminal region of α-synuclein recognized monomers and fibrils almost equally, whereas antibodies to the N-terminal region strongly reacted with fibrils, but labelled monomers only weakly. Under physiological conditions, α-synuclein is known to populate an ensemble of conformations, including conformers that are more compact than expected for a random coil protein [17–19]. Our findings indicating that the N-terminal region is buried and only poorly accessible to antibodies, are in line with this work. They are also in agreement with reports showing that the C-terminal region of α-synuclein is unfolded and shields the N-terminal and central regions by way of long-range intramolecular interactions [13,14].

The core of the fibril spans approximately residues 30–100 of α-synuclein [20,21] and is believed to comprise five parallel β-strands that are separated by flexible loops [16]. Our findings on α-synuclein fibrils are consistent with the loop regions being antibody-accessible. Conformational changes detectable by specific antibodies have previously been reported in tau, another natively unfolded protein, as it assembles into abnormal filaments. Thus, antibody Alz50 reacts more strongly with paired helical filament tau from Alzheimer's disease brain than with the soluble monomeric protein [22].

Inhibitor-bound dimers and monomers of α-synuclein were tested using the same panel of antibodies. When bound to the polyphenol exifone, dimers of α-synuclein were detected by antibodies to the N-terminal region in a manner similar to fibrils. Unlike the latter, inhibitor-bound dimers were not recognized by antibodies to the middle region of α-synuclein. Antibodies to the C-terminal region recognized inhibitor-bound dimers and fibrils equally. Relative to unbound monomers, therefore, inhibitor-bound α-synuclein dimers are characterized by a more accessible N-terminal region. NMR spectroscopy of exifone-stabilized α-synuclein dimers and nitroblue tetrazolium staining of cleaved exifone-bound α-

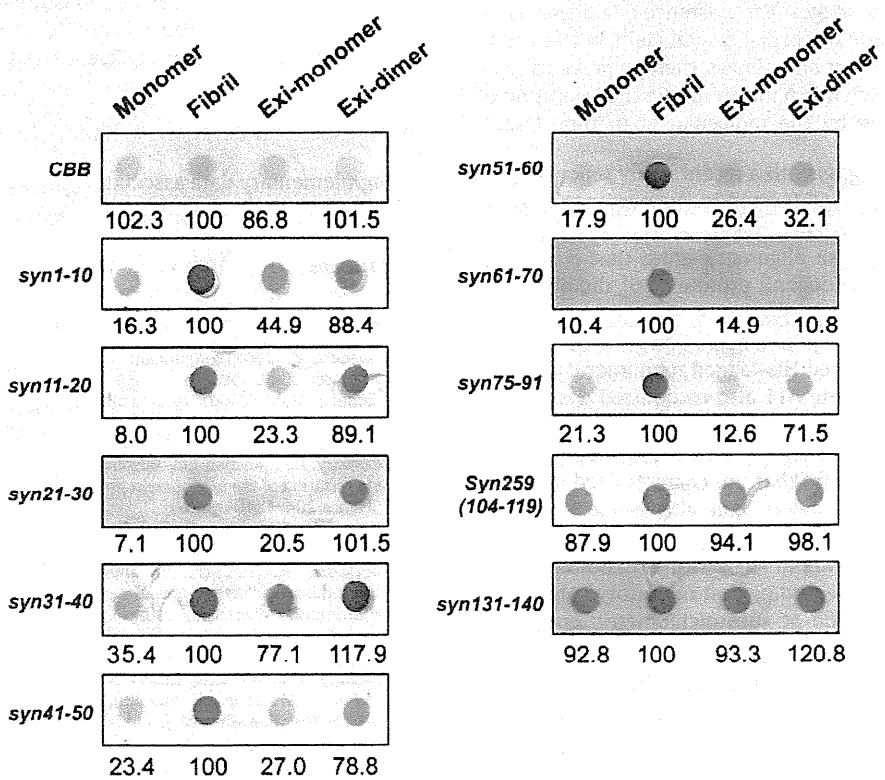

Fig. 2. Dot blot analysis of monomeric α-synuclein, the α-synuclein fibril, as well as exifone-stabilized α-synuclein monomers (Exi-monomer) and dimers (Exi-dimer), with 10 antibodies whose epitopes span the whole of human α-synuclein. The relative intensities of immunoreactivity are indicated below the dots and expressed as % of fibril immunoreactivity (taken as 100, $n = 3$). Each dot corresponds o 100 ng of α-synuclein.

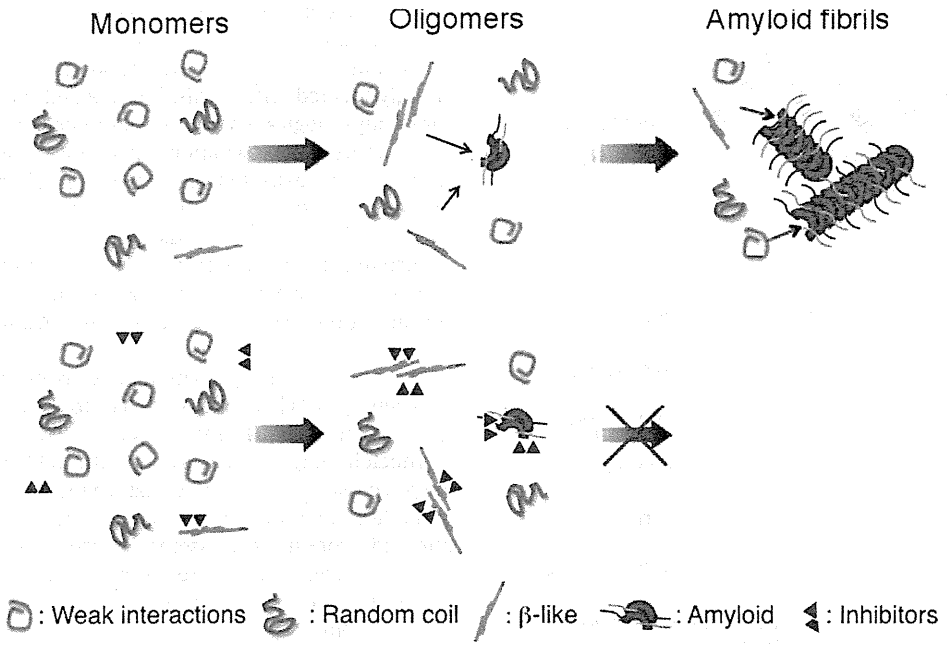

Fig. 3. Model of the inhibition of α-synuclein fibril formation by small molecules.

synuclein showed that N-terminal regions are involved in dimer formation and that exifone binds to these regions (in preparation). Dimers of α-synuclein are believed to play a key role in the aggregation process [23]. A recent study has also shown that aggregation-inhibiting molecules interact with N-terminal regions of α-synuclein [24]. When tested with the panel of antibodies, inhibitor-bound monomers of α-synuclein gave a pattern intermediate between that of unbound monomers and inhibitor-bound dimers. Taken together, our findings suggest the existence of a linear pathway leading from monomeric to fibrillar α-synuclein, with exifone binding to misfolded monomers and dimers, thereby preventing fibril formation. A similar mechanism may underlie the inhibition of α-synuclein fibril formation by the molecular chaperone Hsp70 [25].

This interpretation is at odds with a recent study reporting that oligomers of α-synuclein and Aβ formed in the presence of EGCG were off-pathway [11]. In this study, conformation-specific antibody A11, which recognizes an oligomeric state that is believed to be common to many amyloidogenic proteins [26], did not detect EGCG-induced oligomers. This antibody is believed to be specific for on-pathway toxic oligomers of α-synuclein. However, Ehrnhoefer et al. found that it recognized His-tagged monomeric α-synuclein [11]. In our hands, antibody A11 also recognized α-synuclein fibrils (unpublished observation).

Single molecule studies have shown that α-synuclein exists as three distinct conformers *in vitro* that are characterized by: long-distance weak interactions, random coil and β-like structures [27]. The β-like conformer has been linked to the process of α-synuclein aggregation. It is tempting to suggest that exifone binds to this conformer, in line with the finding that inhibitory compounds inhibit amyloid fibril formation at substoichiometric concentrations [8,9]. Our previous work on the ordered aggregation of tau protein has also shown that small molecule inhibitors bind to oligomers and filaments, but not to native monomers [8]. A revised model for the inhibition of α-synuclein fibril formation by small molecules is shown in Fig. 3. Monomeric α-synuclein exists in a native conformation, with a small proportion of β-like structure. During assembly, the latter may dimerize, oligomerize and form amyloid seeds. Amyloid fibrils can grow from these seeds. Small molecule inhibitors bind to misfolded monomers, dimers and oligomers, thus preventing fibril formation.

Acknowledgements

This work was supported by a Grant-in-aid for Scientific Research on Priority Areas – Research on Pathomechanisms of Brain Disorders (to M.H., 20023038) and Grants-in-aid for Scientific Research (B) (to M.H., 18300117) and (C) (to T.N.) from the Ministry of Education, Culture, Sports, Science and Technology of Japan.

Appendix A. Supplementary data

Supplementary data associated with this article can be found, in the online version, at doi:10.1016/j.febslet.2009.01.037.

References

[1] Goedert, M. and Spillantini, M.G. (2006) A century of Alzheimer's disease. Science 314, 777–781.
[2] Goedert, M. (2001) α-Synuclein and neurodegenerative diseases. Nature Rev. Neurosci. 2, 492–501.
[3] Findeis, M.A. (2000) Approaches to discovery and characterization of inhibitors of amyloid β-peptide polymerization. Biochim. Biophys. Acta 1502, 76–84.
[4] Conway, K.A., Rochet, J.C., Bieganski, R.M. and Lansbury, P.T. (2001) Kinetic stabilization of the α-synuclein protofibril by a dopamine-α-synuclein adduct. Science 294, 1346–1349.
[5] Heiser, V., Engemann, S., Bröcker, W., Dunkel, I., Boeddrich, A., Waelter, S., Nordhoff, E., Lurz, R., Schugardt, N., Rautenberg, S., Herhaus, C., Barnickel, G., Böttcher, H., Lehrach, H. and Wanker, E.E. (2002) Identification of benzothiazoles as potential polyglutamine aggregation inhibitors of Huntington's disease by using an automated filter retardation assay. Proc. Natl. Acad. Sci. USA 99, 16400–16406.
[6] Cashman, N.R. and Caughey, B. (2004) Prion diseases: close to effective therapy? Nat. Rev. Drug Discov. 3, 874–884.
[7] Pickhardt, M., Gazova, Z., von Bergen, M., Khlistunova, I., Wang, Y., Hascher, A., Mandelkow, E.M., Biernat, J. and Mandelkow, E. (2005) Anthraquinones inhibit tau aggregation and dissolve Alzheimer's paired helical filaments *in vitro* and in cells. J. Biol. Chem. 280, 3628–3635.
[8] Taniguchi, S., Suzuki, N., Masuda, M., Hisanaga, S., Iwatsubo, T., Goedert, M. and Hasegawa, M. (2005) Inhibition of heparin-induced tau filament formation by phenothiazines, polyphenols, and porphyrins. J. Biol. Chem. 280, 7614–7623.

[9] Masuda, M., Suzuki, N., Taniguchi, S., Oikawa, T., Nonaka, T., Iwatsubo, T., Hisanaga, S.-I., Goedert, M. and Hasegawa, M. (2006) Small molecule inhibitors of α-synuclein filament assembly. Biochemistry 45, 6085–6094.
[10] Hong, D.-P., Fink, A.L. and Uversky, V.N. (2008) Structural characteristics of α-synuclein oligomers stabilized by the flavonoid baicalein. J. Mol. Biol. 383, 214–223.
[11] Ehrnhoefer, D.E., Bieschke, J., Boeddrich, A., Herbst, M., Masino, L., Lurz, R., Engemann, S., Pastore, A. and Wanker, E.E. (2008) EGCG redirects amyloidogenic polypeptides into unstructured, off-pathway oligomers. Nat. Struct. Mol. Biol. 15, 558–566.
[12] Masuda, M., Dohmae, N., Nonaka, T., Oikawa, T., Hisanaga, S.-I., Goedert, M. and Hasegawa, M. (2006) Cysteine misincorporation in bacterially expressed human α-synuclein. FEBS Lett. 580, 1775–1779.
[13] Dedmon, M.M., Lindorff-Larsen, K., Christodoulou, J., Vendruscolo, M. and Dobson, C.M. (2005) Mapping long-range interactions in α-synuclein using spin-label NMR and ensemble molecular dynamics simulations. J. Am. Chem. Soc. 127, 476–477.
[14] Bertoncini, C.W., Jung, Y.S., Fernandez, C.O., Hoyer, W., Griesinger, C., Jovin, T.M. and Zweckstetter, M. (2005) Release of long-range tertiary interactions potentiates aggregation of natively unstructured α-synuclein. Proc. Natl. Acad. Sci. USA 102, 1430–1435.
[15] Heise, H., Hoyer, W., Becker, S., Andronesi, O.C., Riedel, D. and Baldus, M. (2005) Molecular-level secondary structure, polymorphism, and dynamics of full-length α-synuclein fibrils studied by solid-state NMR. Proc. Natl. Acad. Sci. USA 102, 15871–15876.
[16] Vilar, M., Chou, H.-T., Lührs, T., Maji, S.K., Riek-Loher, D., Verel, R., Manning, G., Stahlberg, H. and Riek, R. (2008) The fold of α-synuclein fibrils. Proc. Natl. Acad. Sci. USA 105, 8637–8642.
[17] Syme, C.D., Blanch, E.W., Holt, C., Jakes, R., Goedert, M., Hecht, L. and Barron, L.D. (2001) A Raman optical activity study of rheomorphism in caseins, synucleins and tau: New insight into the structure and behaviour of natively unfolded proteins. Eur. J. Biochem. 269, 148–156.
[18] Maiti, N.C., Apetrui, M.M., Zagorski, M.G., Carey, P.R. and Anderson, V.R. (2004) Raman spectroscopic characterization of secondary structure in natively unfolded proteins: α-Synuclein. J. Am. Chem. Soc. 126, 2399–2408.
[19] Lee, J.C., Langen, R., Hummal, P.A., Gray, H.B. and Winkler, J.R. (2004) α-Synuclein structures from fluorescence energy-transfer kinetics: Implications for the role of the protein in Parkinson's disease. Proc. Natl. Acad. Sci. USA 101, 16466–16471.
[20] Miake, H., Mizusawa, H., Iwatsubo, T. and Hasegawa, M. (2002) Biochemical characterization of the core structure of α-synuclein filaments. J. Biol. Chem. 277, 19213–19219.
[21] Der-Sarkissian, A., Jao, C.C., Chen, J. and Langen, R. (2003) Structural organization of α-synuclein fibril structure studied by site-directed spin labeling. J. Biol. Chem. 278, 24970–24979.
[22] Carmel, G., Mager, E.M., Binder, L.I. and Kuret, J. (1996) The structural basis of monoclonal antibody Alz50's selectivity for Alzheimer's disease pathology. J. Biol. Chem. 271, 32789–32795.
[23] Yu, J., Malkova, S. and Lyubchenko, Y.L. (2008) α-Synuclein misfolding: single molecule AFM force spectroscopy study. J. Mol. Biol. 384, 992–1001.
[24] Rao, J.N., Dua, V. and Ulmer, T.S. (2008) Characterization of α-synuclein interactions with selected aggregation-inhibiting small molecules. Biochemistry 47, 4651–4656.
[25] Luk, K.C., Mills, I.P., Trojanowski, J.Q. and Lee, V.M.-Y. (2008) Interactions between Hsp70 and the hydrophobic core of α-synuclein inhibit fibril assembly. Biochemistry 47, 12614–12625.
[26] Kayed, R., Head, E., Thompson, J.L., McIntire, T.M., Milton, S.C., Cotman, C.W. and Glabe, C.G. (2003) Common structure of soluble amyloid oligomers implies common mechanism of pathogenesis. Science 300, 486–489.
[27] Sandal, M., Valle, F., Tessari, I., Mammi, S., Bergantino, E., Musiani, F., Brucale, M., Bubacco, L. and Samori, B. (2008) Conformational equilibria in monomeric α-synuclein at the single-molecule level. PLoS Biol. 6, e6.

THE JOURNAL OF BIOLOGICAL CHEMISTRY VOL. 285, NO. 45, pp. 34885–34898, November 5, 2010

Seeded Aggregation and Toxicity of α-Synuclein and Tau

CELLULAR MODELS OF NEURODEGENERATIVE DISEASES[*][S]

Received for publication, May 26, 2010, and in revised form, August 17, 2010 Published, JBC Papers in Press, August 30, 2010, DOI 10.1074/jbc.M110.148460

Takashi Nonaka[‡1], **Sayuri T. Watanabe**[‡§], **Takeshi Iwatsubo**[§¶], **and Masato Hasegawa**[‡2]

From the [‡]*Department of Molecular Neurobiology, Tokyo Institute of Psychiatry, Tokyo 156-8585 and the* [§]*Department of Neuropathology and Neuroscience, Graduate School of Pharmaceutical Science, and* [¶]*Department of Neuropathology, Graduate School of Medicine, University of Tokyo, Tokyo 113-0033, Japan*

The deposition of amyloid-like filaments in the brain is the central event in the pathogenesis of neurodegenerative diseases. Here we report cellular models of intracytoplasmic inclusions of α-synuclein, generated by introducing nucleation seeds into SH-SY5Y cells with a transfection reagent. Upon introduction of preformed seeds into cells overexpressing α-synuclein, abundant, highly filamentous α-synuclein-positive inclusions, which are extensively phosphorylated and ubiquitinated and partially thioflavin-positive, were formed within the cells. SH-SY5Y cells that formed such inclusions underwent cell death, which was blocked by small molecular compounds that inhibit β-sheet formation. Similar seed-dependent aggregation was observed in cells expressing four-repeat Tau by introducing four-repeat Tau fibrils but not three-repeat Tau fibrils or α-synuclein fibrils. No aggregate formation was observed in cells overexpressing three-repeat Tau upon treatment with four-repeat Tau fibrils. Our cellular models thus provide evidence of nucleation-dependent and protein-specific polymerization of intracellular amyloid-like proteins in cultured cells.

The conversion of certain soluble peptides and proteins into insoluble filaments or misfolded amyloid proteins is believed to be the central event in the etiology of a majority of neurodegenerative diseases (1–4). Alzheimer disease (AD)[3] is characterized by the deposition of two kinds of filamentous aggregates, extracellular deposits of β-amyloid plaques composed of amyloid β (Aβ) peptides, and intracellular neurofibrillary lesions consisting of hyperphosphorylated Tau. In Parkinson disease (PD) and dementia with Lewy bodies (DLB), filamentous inclusions consisting of hyperphosphorylated α-synuclein (α-syn) are accumulated in degenerating neurons (5). The deposition of prion proteins in synapses and extracellular spaces is the defining characteristic of Creutzfeldt-Jakob disease and other prion diseases (3). The identification of genetic defects associated with early onset AD, familial PD, frontotemporal dementia, parkinsonism linked to chromosome 17 (caused by Tau mutation and deposition), and familial Creutzfeldt-Jakob disease has led to the hypothesis that the production and aggregation of these proteins are central to the development of neurodegeneration. Fibrils formed of Aβ display a prototypical cross-β-structure characteristic of amyloid (6), as do many other types of filaments deposited in the extracellular space in systemic or organ-specific amyloidoses (7), including prion protein deposits (8). Filaments assembled from α-syn (9) and from Tau filaments (10) were also shown to possess cross-β-structure, as were synthetic filaments derived from exon 1 of huntingtin with 51 glutamines (11). It therefore seems appropriate to consider neurodegenerative disorders developing intracellular deposits of amyloid-like proteins as brain amyloidosis. The accumulation and propagation of extracellular amyloid proteins are believed to occur through nucleation-dependent polymerization (12, 13). However, it has been difficult to establish the relevance of this process in the *in vivo* situation because of the lack of a suitable cell culture model or method to effectively introduce seeds into cells. For example, it has not yet been possible to generate *bona fide* fibrous inclusions reminiscent of Lewy bodies as a model of PD by overexpressing α-syn in neurons of transgenic animals. Here, we describe a novel method for introducing amyloid seeds into cultured cells using lipofection, and we present experimental evidence of seed-dependent polymerization of α-syn, leading to the formation of filamentous protein deposits and cell death. This was also clearly demonstrated in cells expressing different Tau isoforms by introducing the corresponding Tau fibril seeds.

EXPERIMENTAL PROCEDURES

Chemicals and Antibodies—A phosphorylation-independent antibody Syn102 and monoclonal and polyclonal antibodies against a synthetic phosphopeptide of α-syn (Ser(P)[129]) were used as described previously (5). Polyclonal anti-ubiquitin antibody was obtained from Dako. Polyclonal anti-Tau Ser(P)[396] was obtained from Calbiochem. Monoclonal anti-α-tubulin and anti-HA clone HA-7 were obtained from Sigma. Lipofectamine was purchased from Invitrogen. Monoclonal

* This work was supported by grants-in-aid for scientific research on Priority Areas, Research on Pathomechanisms of Brain Disorders (to T. I. and M. H.) and Grant-in-aid for Scientific Research (C) 19590297 and 22500345 (to T. N.) from the Ministry of Education, Culture, Sports, Science, and Technology of Japan.

[S] The on-line version of this article (available at http://www.jbc.org) contains supplemental Figs. S1–S5.

[1] To whom correspondence may be addressed: Dept. of Molecular Neurobiology, Tokyo Institute of Psychiatry 2-1-8 Kamikitazawa, Setagaya-ku, Tokyo 156-8585, Japan. Tel.: 81-3-3304-5701; Fax: 81-3-3329-8035; E-mail: nonaka-tk@igakuken.or.jp.

[2] To whom correspondence may be addressed: Dept. of Molecular Neurobiology, Tokyo Institute of Psychiatry 2-1-8 Kamikitazawa, Setagaya-ku, Tokyo 156-8585, Japan. Tel.: 81-3-3304-5701; Fax: 81-3-3329-8035; E-mail: hasegawa-ms@igakuken.or.jp.

[3] The abbreviations used are: AD, Alzheimer disease; Aβ, amyloid β; PD, Parkinson disease; DLB, dementia with Lewy bodies; α-syn, α-synuclein; 3R1N, three-repeat Tau isoform with one amino-terminal insert; 4R1N, four-repeat Tau isoform with one amino-terminal insert; LA, Lipofectamine; LDH, lactate dehydrogenase.

anti-Tau T46 was from Zymed Laboratories Inc.. AT100 and HT7 antibodies were obtained from Innogenetics.

Preparation of α-Syn Seed, Oligomers, and Tau Fibrils—Human α-syn cDNA in bacterial expression plasmid pRK172 was used to produce recombinant protein (14). Wild-type (WT) or carboxyl-terminally HA-tagged α-syn was expressed in *Escherichia coli* BL21 (DE3) and purified as described (15). To obtain α-syn fibrils, α-syn (5–10 mg/ml) was incubated at 37 °C for 4 days with continuous shaking. The samples were diluted with 5 volumes of 30 mM Tris-HCl buffer (pH 7.5) and ultracentrifuged at 110,000 × *g* for 20 min at 25 °C. The pellets were resuspended in 30 mM Tris-HCl buffer (pH 7.5) and sonicated twice for 5 s each. The protein concentration was determined as described, and this preparation was used as Seed αS. In the case of α-syn oligomers, α-syn (10 mg/ml) was incubated at 37 °C for 3 days in the presence of 10 mM exifone. After incubation, the mixture was ultracentrifuged at 110,000 × *g* for 20 min at 25 °C. The supernatant was desalted by Sephadex G-25 (Amersham Biosciences) column chromatography, and eluted fractions (α-syn oligomers) were analyzed by reversed-phase HPLC, SDS-PAGE, and immunoblot analysis. Recombinant human three-repeat Tau isoform with one amino-terminal insert (3R1N) and four-repeat Tau isoform with one amino-terminal insert (4R1N) monomer and corresponding fibrils were prepared as described previously (16, 17).

Introduction of Proteins into Cells—Human neuroblastoma SH-SY5Y cells obtained from ATCC were cultured in DMEM/F-12 medium with 10% FCS. Cells at ~30–50% confluence in 6-well plates were treated with 200 μl of Opti-MEM containing 2 μg of the seed α-syn WT (Seed αS); HA-tagged α-syn (Seed-HA); α-syn monomers, oligomers; or Tau 3R1N or 4R1N fibrils; and 5 μl of Lipofectamine (LA) for 3 h at 37 °C. The medium was changed to DMEM/F-12, and culture was continued for 14 h. The cells were collected by treatment with 0.5 ml of 0.25% trypsin for 10 min at 37 °C, followed by centrifugation (1,800 × *g*, 5 min) and washing with PBS. The cellular proteins were extracted with 100 μl of homogenization buffer containing 50 mM Tris-HCl, pH 7.5, 0.15 M NaCl, 5 mM EDTA, and a mixture of protease inhibitors by sonication. After ultracentrifugation at 290,000 × *g* for 20 min at 4 °C, the supernatant was collected as a Tris-soluble fraction, and the protein concentration was determined by BCA assay. The pellet was solubilized in 100 μl of SDS-sample buffer. Both Tris-soluble and insoluble fractions were analyzed by immunoblotting with appropriate antibodies as indicated (15, 18).

Cell Culture Model of Seed-dependent Polymerization of α-Syn or Tau—α-Syn or Tau 3R1N or 4R1N was transiently overexpressed in SH-SY5Y cells by transfection of 1 μg of wild-type human α-syn cDNA in pcDNA3 (pcDNA3-α-syn) or human Tau cDNA in pcDNA3 (pcDNA3-Tau 3R1N or 4R1N) with 3 μl of FuGENE6 (Roche Applied Science) in 100 μl of Opti-MEM, followed by culture for 14 h. Under our experimental conditions, the efficiency of transfection with pEGFP-C1 vector was 20–30%. The cells were washed with PBS once, and then Seed αS, Seed-HA, Seed 3R1N, or Seed 4R1N was introduced with Lipofectamine as described above. The medium was changed to DMEM/F-12, and culture was continued for ~2–3 days. Cells were harvested in the presence of trypsin to digest extracellular cell-associated α-syn fibrils. The cellular proteins were differentially extracted and immunoblotted with the indicated antibodies, as described (18).

Confocal Microscopy—SH-SY5Y cells on coverslips were transfected with pcDNA3-α-syn and cultured for 14 h as described above, and then Seed αS was introduced, and culture was continued for ~1–2 days. After fixation with 4% paraformaldehyde, the cells were stained with appropriate primary and secondary antibodies as described previously (18). For thioflavin S staining, the cells were incubated with 0.05% thioflavin S at room temperature for 5 min. Fluorescence was analyzed with a laser-scanning confocal fluorescence microscope (LSM5Pascal, Carl Zeiss).

Immunoelectron Microscopy—For electron microscopy, cells overexpressing α-syn were transfected with Seed αS, cultured for 2 days, fixed in 0.1 M phosphate buffer containing 4% glutaraldehyde for 12 h, and then processed and embedded in LR White resin (London Resin, Reading, UK). Ultrathin sections were stained with uranyl acetate for investigation. Immunolabeling of the inclusions was performed by means of an immunogold-based postembedding procedure. Sections were blocked with 10% calf serum, incubated overnight on grids with anti-Ser(P)^{129} antibody at a dilution of 1:100, rinsed, then reacted with secondary antibody conjugated to 10-nm gold particles (E-Y Laboratories, San Mateo, CA) (1:10), rinsed again and stained with uranyl acetate.

Immunoelectron microscopic analysis of α-syn or Tau filaments extracted from cells was performed as follows. Cells overexpressing α-syn or Tau were transfected with Seed αS or Seed Tau, respectively. After incubation for 3 days, they were harvested, suspended in 200 μl of 10 mM Tris-HCl, pH 7.4, 1 mM EGTA, 10% sucrose, 0.8 M NaCl) and sonicated. The lysates were centrifuged at 20,400 × *g* for 20 min at 4 °C. The supernatant was recovered, and Sarkosyl was added (final 1%, v/v). The mixtures were incubated at room temperature for 30 min and then centrifuged at 113,000 × *g* for 20 min. The resulting pellets were suspended in 30 mM Tris-HCl, pH 7.5, placed on collodion-coated 300-mesh copper grids, and stained with the indicated antibodies and 2% (v/v) phosphotungstate. Micrographs were recorded on a JEOL 1200EX electron microscope.

Cell Death Assay—Cell death assay was performed using a CytoTox 96 non-radioactive cytotoxicity assay kit (Promega). TUNEL staining was performed using an *in situ* cell death detection kit (Roche Applied Science).

Assay of Proteasome Activity—SH-SY5Y cells transfected with pcDNA3-α-syn and Seed αS were cultured for 3 days or treated with 20 μM MG132 for 4 h. Cells were harvested, and cytosolic fraction was prepared as follows. Cells were resuspended in 100 μl of phosphate-buffered saline (PBS) and disrupted by sonication, and then insoluble material was removed by ultracentrifugation at 290,000 × *g* for 20 min at 4 °C. The supernatant was assayed for proteasome activity by using a fluorescent peptide substrate, benzyloxycarbonyl-Leu-Leu-Glu-7-amido-4-methylcoumarin (Peptide Institute, Inc.). 7-Amino-4-methylcoumarin release was measured fluorometrically (excitation at 365 nm; emission at 460 nm). In a green fluorescent protein (GFP) reporter assay of proteasome activity in living cells by confocal laser microscopy, SH-SY5Y cells trans-

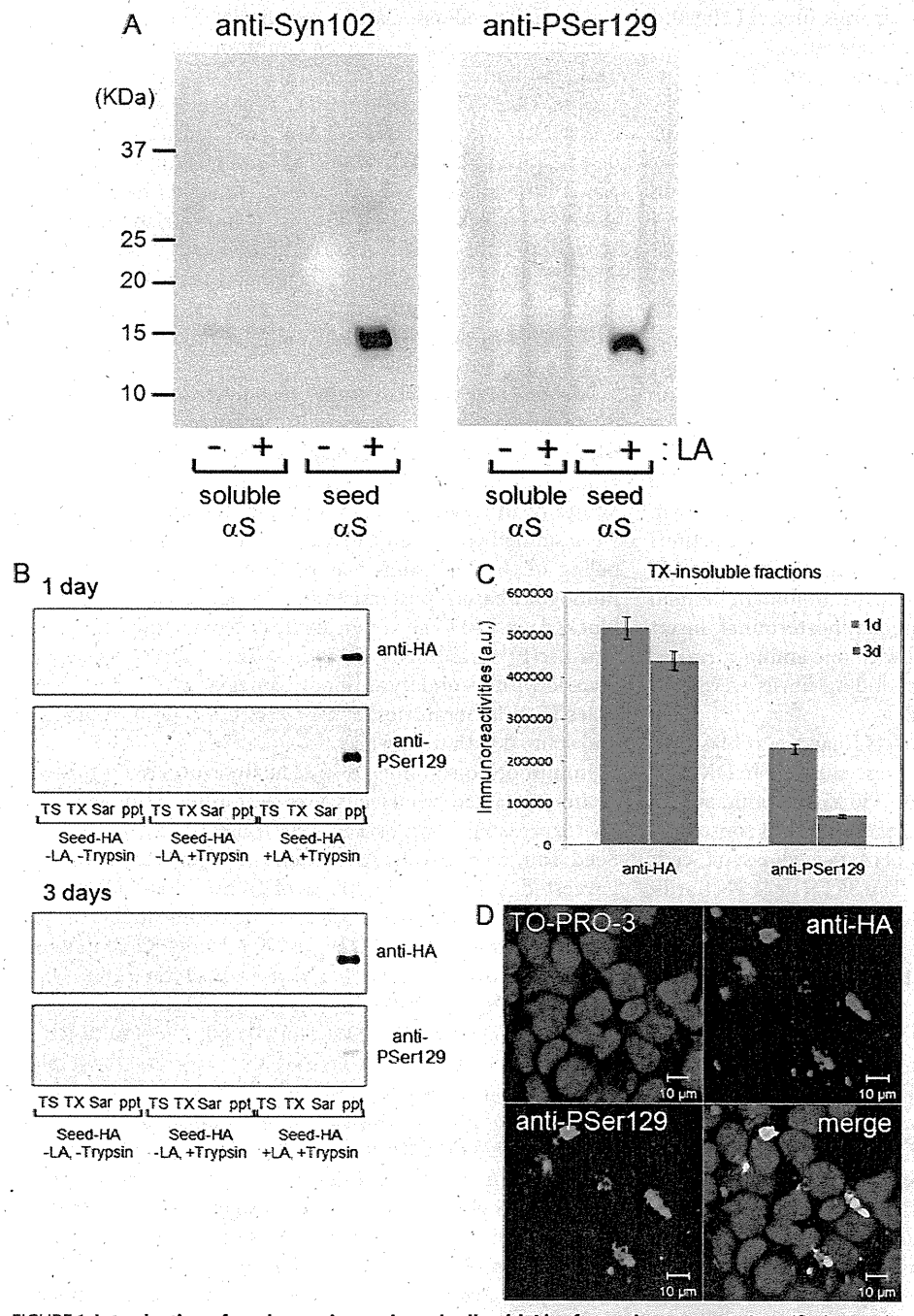

FIGURE 1. **Introduction of seed α-syn into cultured cells with Lipofectamine reagent.** *A*, purified recombinant α-syn (soluble form; 2 μg) and filaments (2 μg) were sonicated and then incubated with LA. The protein-LA complexes were dispersed in Opti-MEM and added to SH-SY5Y cells. After 14 h of culture, the cells were collected and sonicated in SDS sample buffer. After boiling, the samples were analyzed by immunoblotting with a phosphorylation-dependent anti-α-syn Ser(P)^{129} (*PSer129*) (*right*) or a phosphorylation-independent antibody, Syn102 (*left*). *B* and *C*, carboxyl-terminally HA-tagged α-syn fibril seeds (*Seed-HA*) were transduced into cells by the use of LA. After incubation for 1 day (*1d*) or 3 days (*3d*), cells were harvested with or without trypsin, and proteins were differentially extracted from the cells with Tris-HCl (*TS*), Triton X-100 (*TX*), and Sarkosyl (*Sar*), leaving the pellet (*ppt*). Immunoblot analyses of lysates using anti-HA and anti-Ser(P)^{129} are shown. The immunoreactive band positive for anti-HA or anti-Ser(P)^{129} in the Triton X-100-insoluble fraction was quantified. The results are expressed as means ± S.E. ($n = 3$). *D*, confocal laser microscopic analysis of cells treated with Seed-HA in the presence of LA. Cells were transduced with 2 μg of Seed-HA using 5 μl of LA. After a 48-h incubation, cells were fixed and immunostained with anti-Ser(P)^{129} (*green*) and anti-HA (*red*) and counterstained with TO-PRO-3 (*blue*).

fected with pcDNA3-α-syn (1 μg) and GFP-CL1 (0.3 μg) using FuGENE6 and then transfected with Seed αS were grown on coverslips for 2 days or treated with 20 μM MG132 for 6 h (19). These cells were analyzed using a laser-scanning confocal fluorescence microscope (LSM5Pascal, Carl Zeiss).

Statistical Analysis—The *p* values for the description of the statistical significance of differences were calculated by means of the unpaired, two-tailed Student's *t* test using GraphPad Prism 4 software (GraphPad Software).

RESULTS

Introduction of Seed α-Syn into Cultured Cells Using Lipofectamine Reagent—Cellular overexpression of α-syn by itself does not lead to fibrillization of α-syn in a form that resembles Lewy bodies. This prompted us to examine whether or not introduction of preformed aggregation seeds of α-syn (Seed αS) would elicit fibril formation. To introduce Seed αS into SH-SY5Y cells in a non-invasive manner, we tried several reagents used for transporting proteins or plasmid DNA into cells and found that LA, a cationic gene introducer, enables the introduction of Seed αS into SH-SY5Y cells. We were not able to detect any introduced α-syn monomer or fibrils following the simple addition of protein preparations to the culture medium, notwithstanding a previous report on this approach (20). The insoluble α-syn formed following LA-mediated Seed αS introduction was detected as buffer-insoluble α-syn in cell lysates (Fig. 1*A*). The insoluble α-syn was phosphorylated at Ser^{129} upon introduction into cells (Fig. 1*A*), indicating that Seed αS was incorporated in cells and phosphorylated intracellularly. Cells were harvested in the presence of trypsin to digest extracellular cell-associated α-syn fibrils. The optimal ratio of LA to Seed αS was about 5 μl to 2 μg of protein in 6-well plates. This treatment effectively introduced Seed αS not only into SH-SY5Y cells but also into several other types of cells examined, including Chinese hamster ovary cells and human embryonic kidney 293T cells (data not shown). In sharp contrast, soluble α-syn (either monomeric or oligomeric forms) was not introduced into the